Fragmentation of massive dense cores down to ~1000 AU:

characterizing protocluters

Aina Palau
Centro de Radioastronomía y Astrofísica
(UNAM, México)

Fragmentation of massive dense cores down to ~1000 AU

Aina Palau

R. Estalella, G. Busquet, A. Fuente, J. M. Girart, P. T. P. Ho,
B. Commerçon, P. Hennebelle, Á. Sánchez-Monge,
F. Fontani, J. Boissier, Q. Zhang, S. Bontemps,
E. Vázquez-Semadeni, J. Ballesteros-Paredes, L. Zapata

Introduction

Method + First Results

One step forward: density and T

Role of turbulence and B

Cone Nebula and Snowflake cluster, Spitzer, NASA, JPL-Caltech, P. S. Teixeira

How are structures formed within molecular clouds?

turbulence-regulated, quasi-equilibrium scenario (Mac Low & Klessen 04; Vázquez-Semadeni +00)

global-hierarchical chaotic **gravitational** contraction (Hartmann +01; Vázquez-Semadeni 14)

Turbulence-regulated, quasi-equilibrium scenario

✓MCs are globally supported by supersonic turbulence and close to equilibrium

✓MCs evolve in long timescales (several t_{cross})

✓Supersonic turbulence → local compressions → fragments MCs into dense sheets, filaments and cores (highly radiative shocks)

✓Large-scales: turbulence gives support against gravity in addition to thermal support

Turbulence-regulated, quasi-equilibrium scenario

$$\left[\frac{M_{\rm Jeans}^{\rm nth}}{M_\odot}\right] = 1.578 \left[\frac{\sigma_{\rm nth}}{0.188\,{\rm km\,s^{-1}}}\right]^3 \left[\frac{n}{10^5\,{\rm cm^{-3}}}\right]^{-1/2}$$

Chandrasekhar+53

$$\left[\frac{M_{\rm Jeans}^{\rm conv.flows}}{M_\odot}\right] = 1.578 \left[\frac{\sigma_{\rm nth}}{0.188\,{\rm km\,s^{-1}}}\right]^3 \left[\frac{n\,\mathcal{M}^2}{10^5\,{\rm cm^{-3}}}\right]^{-1/2}$$

see Mac Low & Klessen 04

Fragmentation: turbulent-Jeans

✓very few grav. unstable density fluctuations in a core

✓naturally yields massive fragments

Global+hierarchical+chaotic gravitational contraction

✓MCs rapidly evolving (1 t_{cross}), unstable, dynamic struc.

✓Expected from MC formation:

- ✓large-scale compressions in Warm Neutral Medium
- ✓sudden phase transition to Cold NM → M_{Jeans} decreases by 10^4! → ~pressureless **GLOBAL** collapse

✓Amplification of any anisotropy → collapse first along shortest dimension (Lin+65): ellipsoid → sheet → filament

✓Internal turbulence → clumps+cores: cores collapse faster than entire cloud → **HIERARCHICAL and CHAOTIC**

Global+hierarchical+chaotic gravitational contraction

Fragmentation: thermal-Jeans

- ✓efficient to produce low-mass fragments

$$\left[\frac{M_{\rm Jeans}^{\rm th}}{M_{\odot}}\right] = 0.6285 \left[\frac{T}{10\,{\rm K}}\right]^{3/2} \left[\frac{n}{10^5\,{\rm cm}^{-3}}\right]^{-1/2}$$

- ✓formation of massive fragments through
  - ✓accretion from regions not originally bound to the protostellar core
  - ✓radiative feedback?
  - ✓magnetic field? $M_{crit} = M_J + M_\phi = M_J + c_\phi \pi R^2 B/G^{1/2}$

MHD simulations of the collapse of a turbulent and magnetized cloud: higher B supresses fragmentation

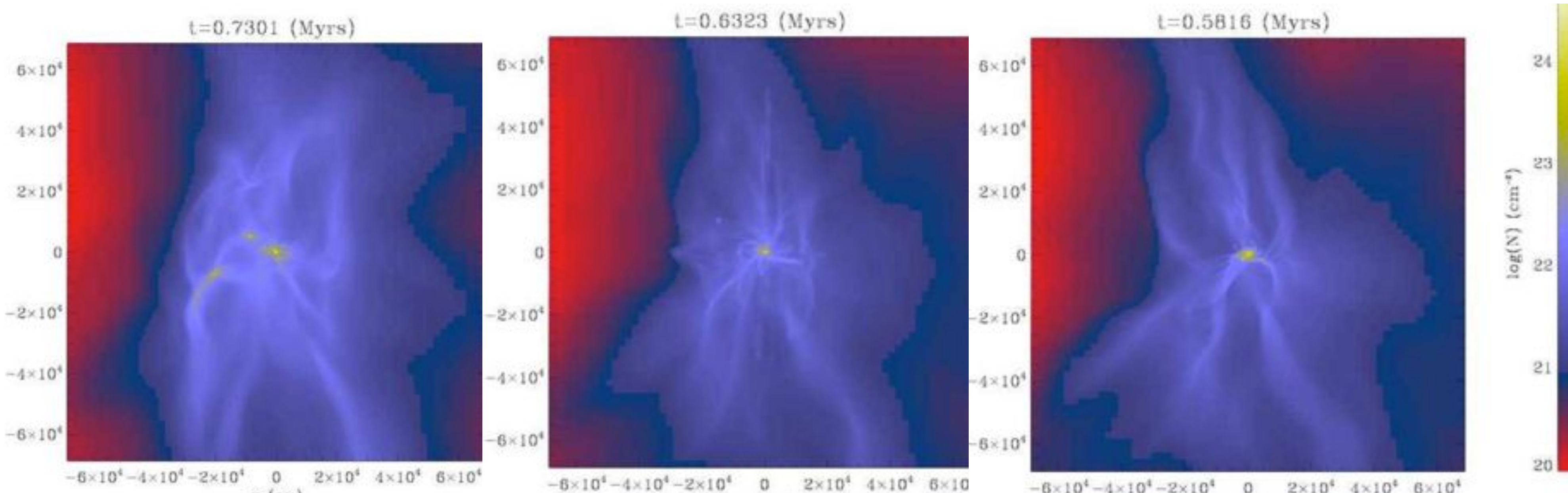

Hennebelle et al. 2011, Commerçon et al. 2011

Increasing magnetization degree

Also: e.g., Vázquez-Semadeni+05,+11, Ziegler+05, Banerjee & Pudritz 06, Price & Bate 07, Peters+11, Myers+13, etc., etc.

Fragmentation can be mainly controlled by:

- ✓turbulence (turb-regulated quasi-equilibr. scenario)
- ✓gravity (global-hierarchical-chaotic grav. contraction)
- ✓role of B and radiative feedback

Is any of these ingredients dominating?

Introduction

Method + First Results

One step forward: density and T

Role of turbulence and B

Lagoon Nebula (M8), Fred Vanderhaven (image processed to remove stars)

Observational approach: fragmentation of massive dense cores

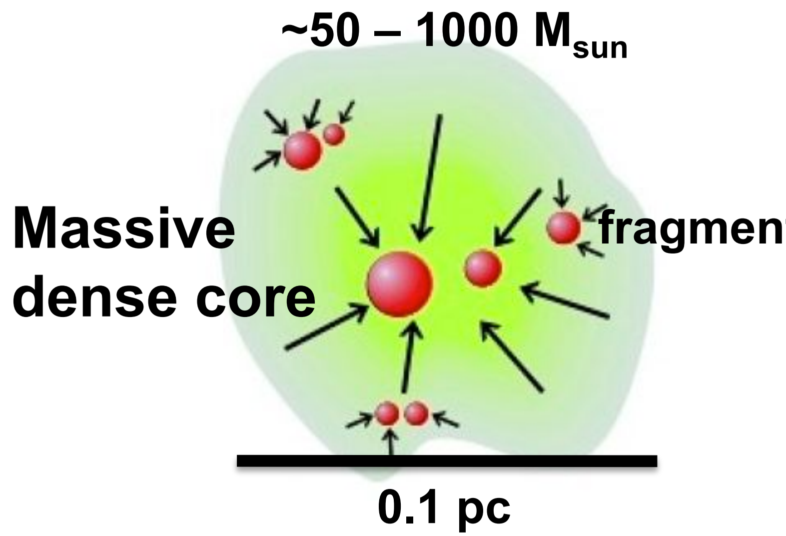

Observe them:

✓down to ~1000 AU

✓down to M_{min}~0.5 M_{sun}

Literature (5 yr ago): massive star-forming regions studied with mm interferometers down to M_{min} ~0.5 M_{sun}

Source	Lbol (Lsun)	D (kpc)	IR data	temptative evol. stage massiveYSO	current spa.resol. (AU)	number of of mm sources	mm/submm interferom.	achievable PdB (0."3) spa.res.(AU)	Visibility issues	Refs
NGC2264-DMM1	108	0.80	IRAC+MIPS	Class 0	1200	7	SMA	240	DEC~+9°	Teixeira et. 2007, ApJ, [illegible]
IRDC 18223-3	177	3.70	IRAC+MIPS	Class 0	4800	4	SMA+PdB	1110	DEC~-12°	Fallscheer et. 2009, A&A, 504,127
IRAS20050+2720	300	0.70	IRAC+MIPS	Class 0/I	4900	3	OVRO	210	Ok	Beltran et. 2008, A&A, 481, 93
IC1396N	440	0.75	IRAC+MIPS	Class 0/I	300	4	PdBe	225	DONE	Neri et. 2007, A&A, 468, 33
IRAS22198+6336	450	0.76	IRAC+MIPS	Class 0	1700	1	SMA+PdB	228	Ok	Sánchez-Monge et., in prep.
NGC7129-FIRS2	500	1.25	IRAC+MIPS	Class 0	1400	1	PdB	375	Ok	Fuente et. 2005, A&A, 444, 481
ISOSSJ18364-0221	800	2.20	IRAC+MIPS	Class 0	>3300	2	PdB	660	DEC~-2°	Hennemann 2009,ApJ,693,1379
CB3	930	2.50	MIPS	Class I	900	2	PdBe	750	Ok	Fuente et. 2007, A&A, 468, 37
IRDC 19175-4/5	<1000	1.10	IRAC+MIPS	Class 0/I	3400	1	PdB	330	DEC~-14°	Beuther et. 2009, A&A, 503, 859
IRAS22272+6358A	1200	0.91	IRAC+MIPS	Class 0/I	4500	2	OVRO	273	Ok	Beltran et. 2006, A&A, 457, 865
IRAS00117+6412	1300	1.80	2MASS only	UCHII, B2	6800	2	PdB+SMA	540	Ok	Palau 2006, PhD thesis, Barcelona
IRAS05345+3157	1400	1.80	IRAC+MIPS	UCHII, B1	5400	3	SMA+PdB	540	Ok	Fontani et. 2008, A&A, 477, L45
IRAS22172+5549	1800	2.40	IRAC+MIPS	pre-UCHII	15600	1	OVRO	720	Ok	Fontani et. 2004, A&A, 424, 179
NGC6334 I(N)	1900	1.70	IRAC+MIPS	B2	3400	7	SMA+ATCA	510	DEC~-35°	Hunter et. 2006, ApJ, 649, 888
IRAS23033+5937	2100	3.50	IRAC+MIPS	Class 0	3500	1	PdB	1050	Ok	Birkmann et. 2007, A&A, 474, 883
G14.2-0.60	2500	2.20	IRAC+MIPS	UCHII	3200	16	SMA	660	DEC~-16°	Busquet et., in prep.
AFGL5142	3000	1.80	IRAC+MIPS	UCHII, B2	2300	3	SMA+CARMA	540	Ok	Zhang et. 2007, ApJ, 658, 1152
OMC-1S	3000	0.45	IRAC+MIPS	Class I, B2	450	6	SMA	135	DONE	Zapata et. 2006, ApJ, 630, L85
IRAS20343+4129	3200	1.40	IRAC+MIPS	CHII, B2	4200	7	SMA	420	Ok	Palau et. 2007, A&A, 474, 911
R Mon	4000	0.80	IRAC	Class I/HBe	390	1	PdB	240	DONE	Fuente et. 2006, ApJ, 649, L119
IRAS21307+5049	4000	3.20	2MASS only	pre-UCHII	20800	2	OVRO	960	Ok	Fontani et. 2004, A&A, 424, 179
IRAS20293+3952	6300	2.00	IRAC+MIPS	UCHII, B1	1200	5	PdB+BIMA	600	Ok	Beuther et. 2004, ApJ, 615, 832
IRAS05358+3543	6300	1.80	IRAC+MIPS	HCHII, B1	1100	5	PdB	540	Ok	Leurini et. 2007, A&A, 475, 925
IRAS20126+4104	7900	1.70	IRAC+MIPS	pre-UCHII	1300	2	PdB	510	Ok	Cesaroni et. 2005, A&A,434 1039
IRAS19410+2336	10000	2.00	IRAC+MIPS	UCHII	2000	11	PdB	600	Sun avoid	Beuther et. 2004, Sci, 303, 1167
G28.53-0.25-MM1	100-10000	3.70	IRAC+MIPS	pre-hot mol core	8100	2	SMA	1110	DEC~-3°	Rathborne et.2008,arXiv:0808.2973
G24.60+0.08-MM1	11000	3.70	IRAC+MIPS	IR dark cloud	6840	4	PdB	1110	DEC~-7°	Rathborne et. 2007,ApJ,662,1082
AFGL 961	11400	1.60	IRAC+MIR	Pre-UCHII	4900	3	SMA	480	DEC~4°	Williams et. 2009, ApJ, 699, 1300
IRAS 20081+3822	12600	1.80	H2	UCHII,B0	1300	4	SMA	540	Ok	Su et. 2009, ApJ, 698, 1981
IRAS22134+5834	12600	2.60	JHKL,MIPS	HCHII	10900	1	CARMA	780	Ok	Sánchez-Monge et., in prep.
OrionBN/KL	25000	0.45	IRAC+MIPS	B0 (BN object)	400	>7	SMA	135	DONE	Beuther et. 2004, ApJ, 616, 31
IRAS18089-1732	32000	3.60	IRAC+MIPS	HCHII	3600	1	SMA	1080	Sun avoid	Beuther et. 2005, ApJ, 628, 800
G34.43+0.24-MM1	32000	3.70	IRAC+MIPS	hot molec core	8100	1	SMA	1110	DEC~+1°	Rathborne et.2008,arXiv:0808.2973
S255N	100000	2.60	IRAC	UCHII	8600	3	SMA	780	DEC~+13°	Cyganowski 2007, ApJ, 134, 346
W28A2	126000	2.00	IRAC+MIPS	UCHII, O5	1800	4	SMA	600	DEC~-24°	Hunter et. 2008, arXiv:0803.0587
NIRS5	200000	1.95	IRAC+MIPS	HCHII	720	4	PdB	585	DONE	Rodón et. 2008, arXiv:0809.0292
NGC6334 I	260000	1.70	IRAC+MIPS	O8.5	2700	4	SMA	510	DEC~-35°	Hunter et. 2006, ApJ, 649, 888

Already 5 regions with ~1000 AU

Select 6 new regions:

✓ < 2.5 kpc

✓ associated with strong mm emission

✓ cover range of L_{bol}

✓ very similar evolutionary stages

Total: ~10 regions

We used most extended “A” configuration → beam ~ 0.4”

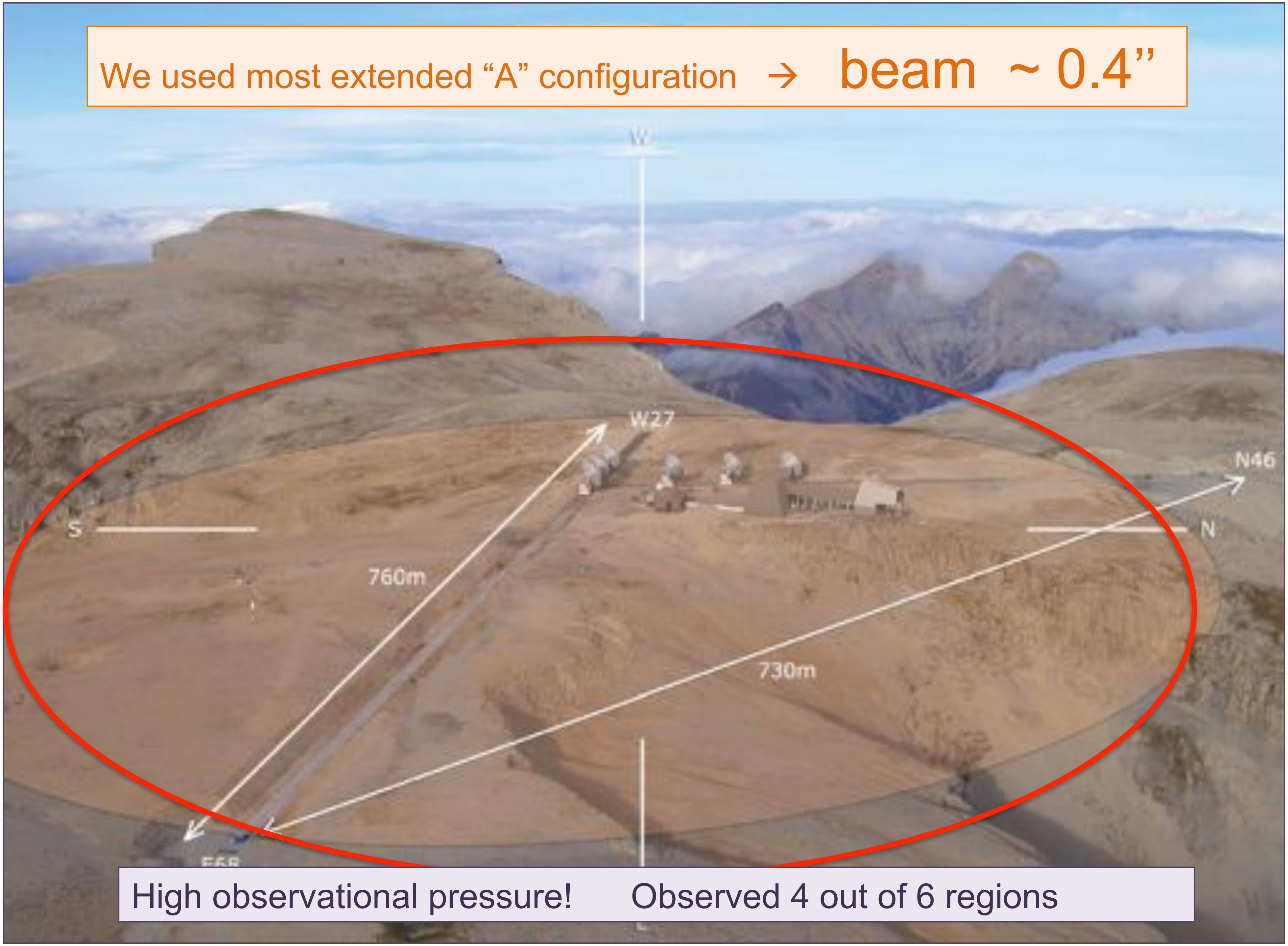

High observational pressure!   Observed 4 out of 6 regions

Single-dish submm/mm continuum archive observations of dense cores of all the sample:

JCMT, Hawaii, USA
SCUBA bolometer 450 & 850 μm
Di Francesco et al. 2008

IRAM30m Granada, Spain
MAMBO bolometer 1.2 mm
Motte et al. 2007

In the meantime: 10 regions more in the literature!
Total: 19 regions (Palau+13, +14, including Bontemps+10)

The Astrophysical Journal, 762:120 (19pp), 2013 January 10 — Palau et al.

Table 3
Massive Dense Cores Studied with Interferometers at 1.3 mm with High Sensitivity and Down to a Spatial Resolution $\lesssim$1000 AU

ID-Source[a]	D (kpc)	L_{bol} ($L_\odot$)	T_{bol}[b] (K)	rms[c] (mJy)	M_{min}[c] ($M_\odot$)	Spat. Res.[d] (AU)	LAS[d] (AU)	N_{mm}[e]	N_{mm+IR}[e]	N_{IR}/N_{mm}	st. dens.[f] (10^4 pc^{-3})	Separation[f] (AU)
1-IC1396N	0.75	290	52	0.52	0.03	340	900	4	8	1.00	69	1800
2-I22198	0.76	340	59	2.0	0.13	300	700	1.5	2	0.33	3	...
3-NGC 2071-IRS1[g]	0.42	440	98	0.50	0.20	200	5500	4	14	2.50	16	2900
4-NGC 7129-FIRS2	1.25	460	58	2.9	0.49	750	1500	1	2	1.00	3	...
5-CB3-mm	2.50	700	49	0.43	0.29	875	2500	2	$\gtrsim$2	$\gtrsim$0.00	$\gtrsim$3	...
6-I22172N-IRS1	2.40	830	195	0.55	0.34	1000	2100	3	6	1.00	6	4400
7-OMC-1S-136	0.45	2000	...	30	0.66	540	3300	9	21	1.33	9	3000
8-A5142	1.80	2200	55	2.8	0.99	700	1600	7	11	0.57	7	3700
9-I05358+3543NE	1.80	3100	67	1.5	0.53	900	2100	4	7	0.75	10	3500
10-I20126+4104	1.64	8900	61	2.6	0.76	1400	4000	1	3	2.00	23	2700
11-I22134-IRS1	2.60	11800	93	0.30	0.22	1300	2300	3.5	7	1.00	4	4600
12-HH80-81	1.70	21900	81	3.0	0.94	830	4000	3	6	1.00	6	4200
13-W3IRS5	1.95	140000	114	1.2	0.50	720	2300	3.5	$\gtrsim$5.5	$\gtrsim$0.57	$\gtrsim$46	2300
14-AFGL 2591	3.00	190000	226	0.51	0.49	1000	1900	1.5	$\gtrsim$1.5	$\gtrsim$0.00	$\gtrsim$3	...
15-CygX-N53	1.40	300	33	1.9	0.41	1400	6900	4	7	0.75	11	3400
16-CygX-N12	1.40	320	58	1.9	0.41	1400	6900	2.5	5	1.00	23	2800
17-CygX-N63	1.40	470	39	4.2	0.90	1400	6900	2.5	4	0.60	72	2000
18-CygX-N48	1.40	4400	48	2.2	0.47	1400	6900	4	5	0.25	11	3600

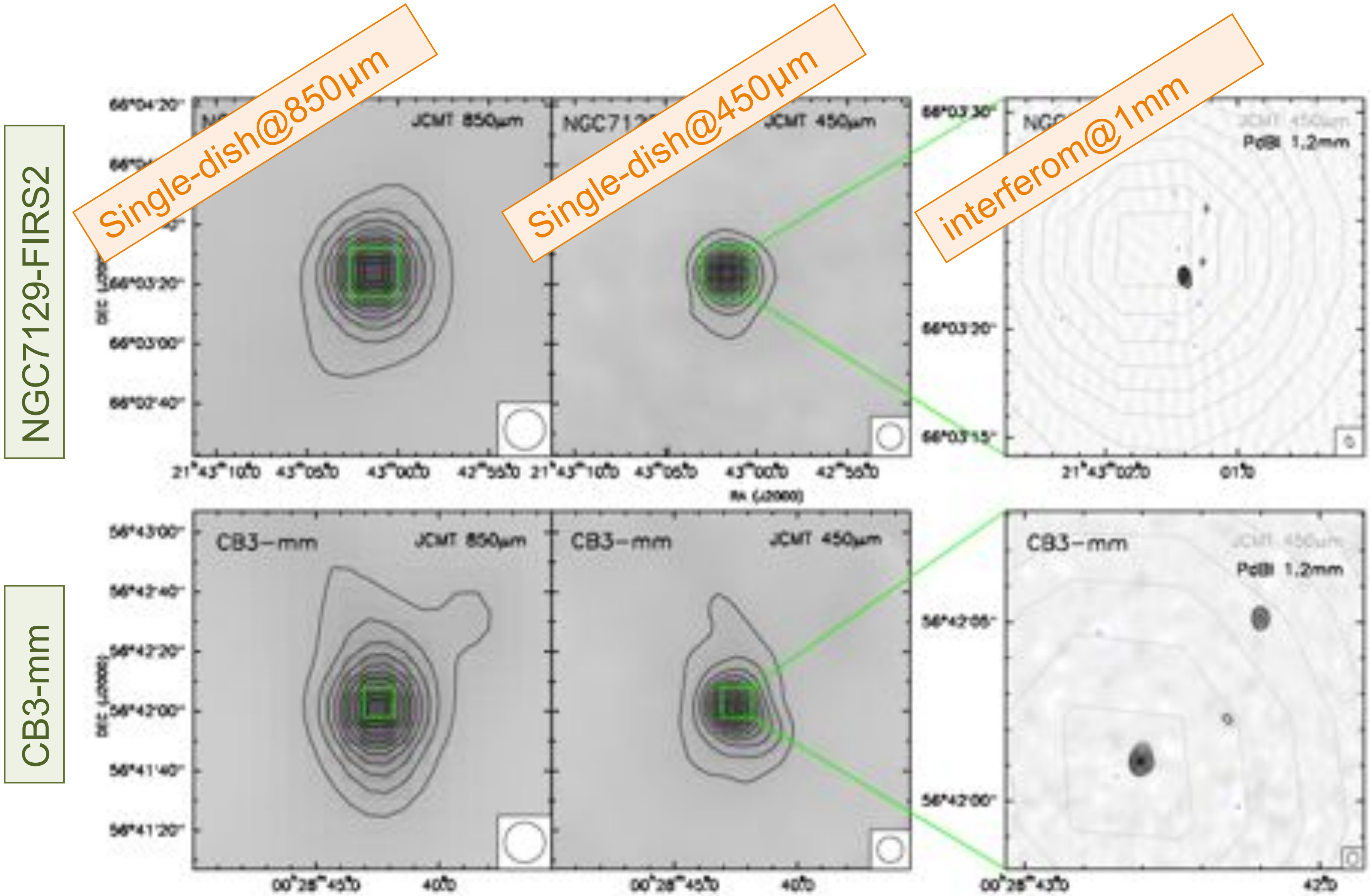

NGC7129-FIRS2
CB3-mm
Single-dish@850μm
Single-dish@450μm
interferom@1mm
JCMT 850μm
JCMT 450μm
PdBI 1.2mm
CB3−mm
CB3−mm
CB3−mm
JCMT 850μm
JCMT 450μm
PdBI 1.2mm

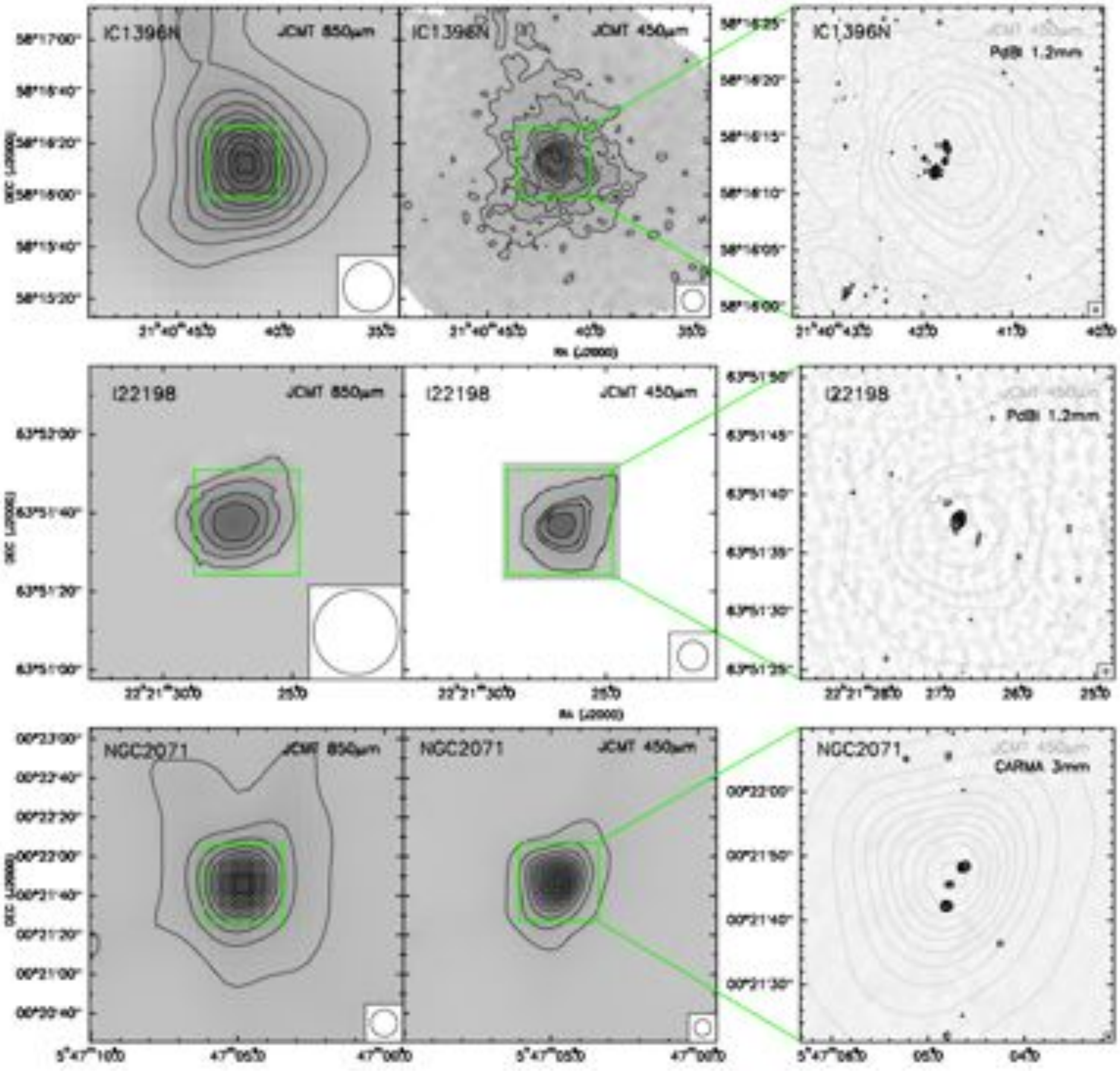
IC1396N
JCMT 850μm
JCMT 450μm
PdBI 1.2mm
I22198
NGC2071
CARMA 3mm
DEC (J2000)
RA (J2000)

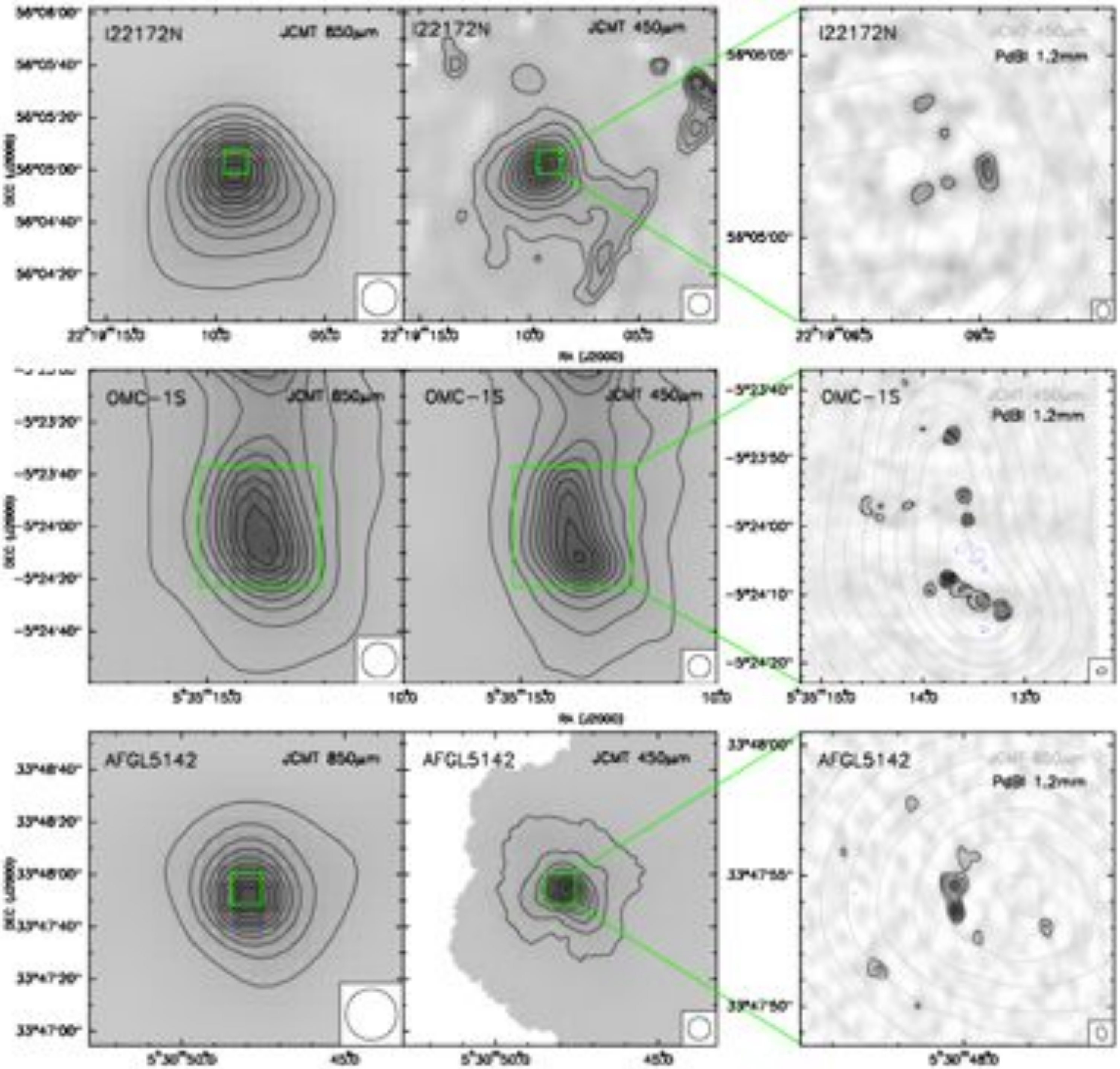
I22172N
JCMT 850μm
I22172N
JCMT 450μm
I22172N
PdBI 1.2mm
OMC-1S
JCMT 850μm
OMC-1S
JCMT 450μm
OMC-1S
PdBI 1.2mm
AFGL5142
JCMT 850μm
AFGL5142
JCMT 450μm
AFGL5142
PdBI 1.2mm

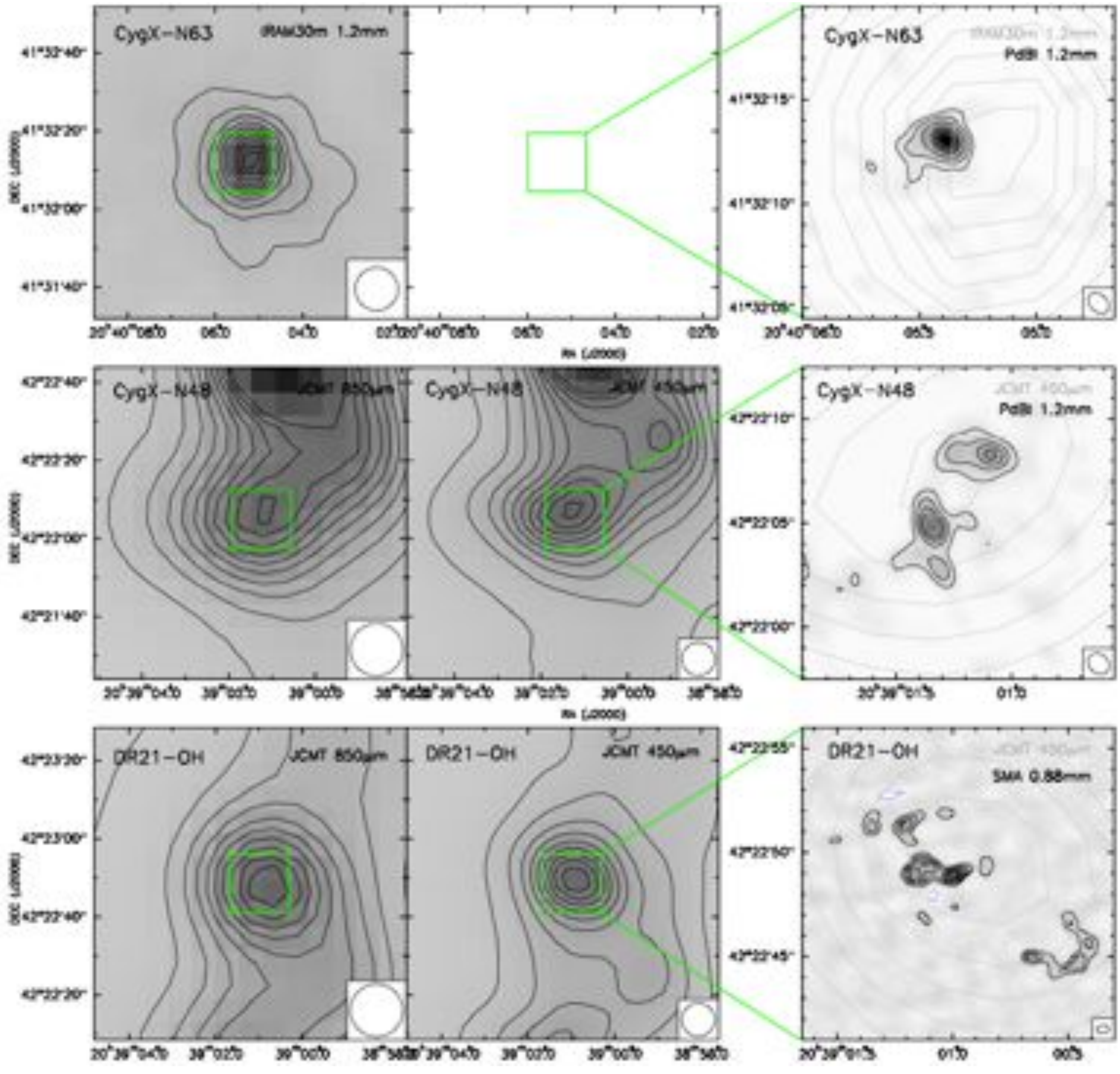
CygX-N63
IRAM30m 1.2mm
CygX-N63
PdBI 1.2mm
CygX-N48
JCMT 850μm
CygX-N48
JCMT 450μm
CygX-N48
PdBI 1.2mm
DR21-OH
JCMT 850μm
DR21-OH
JCMT 450μm
DR21-OH
SMA 0.88mm

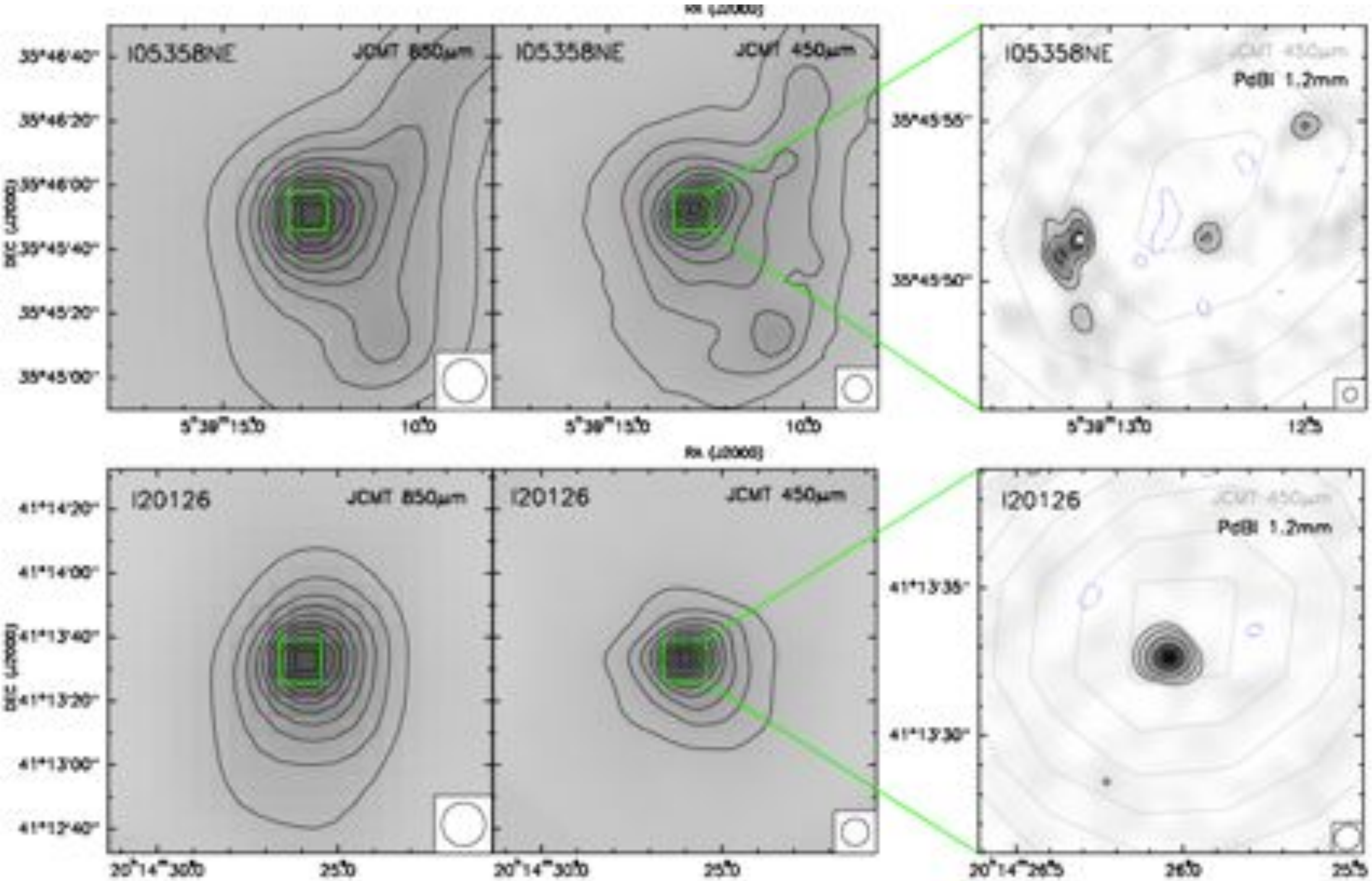

I05358NE
JCMT 850μm
JCMT 450μm
PdBI 1.2mm
I20126
RA (J2000)
DEC (J2000)

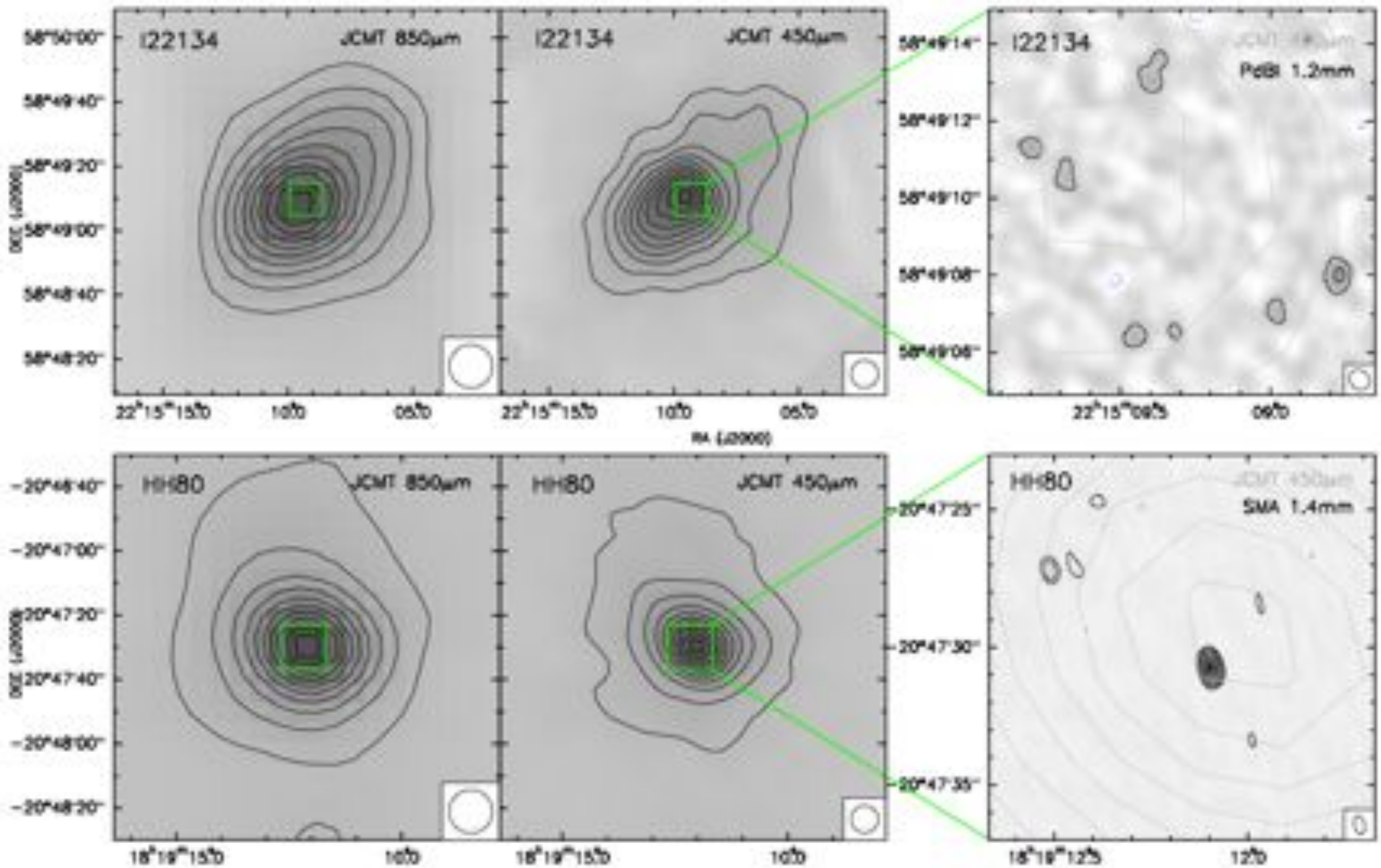

I22134
JCMT 850μm
I22134
JCMT 450μm
I22134
PdBI 1.2mm
HH80
JCMT 850μm
HH80
JCMT 450μm
HH80
JCMT 450μm
SMA 1.4mm
RA (J2000)
DEC (J2000)

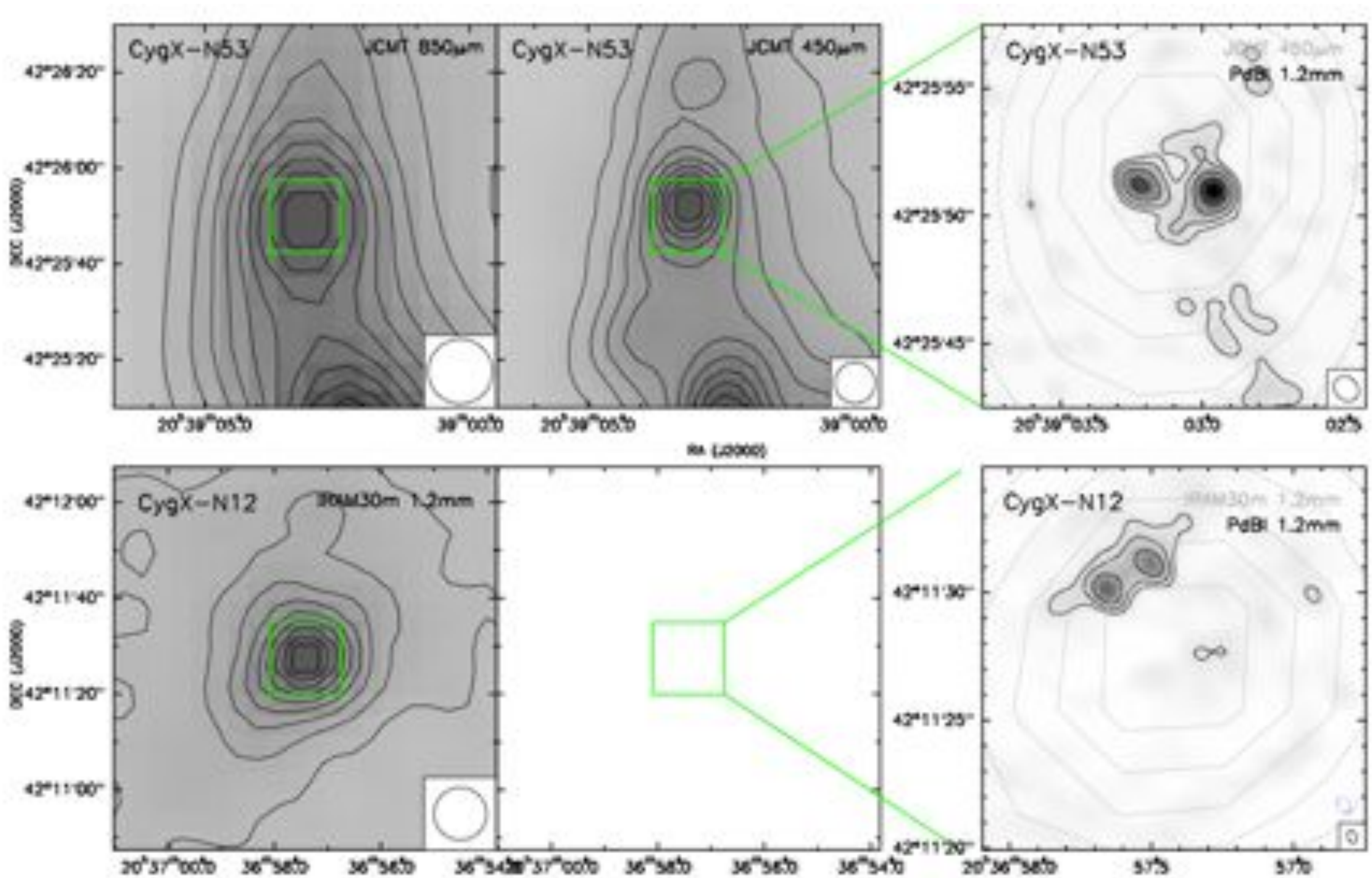

CygX-N53
JCMT 850μm
JCMT 450μm
PdBI 1.2mm
CygX-N12
IRAM30m 1.2mm
DEC (J2000)
RA (J2000)

~30% low fragmentation level: 1 source dominating
~50% high fragmentation: split up into ~4 fragments or more

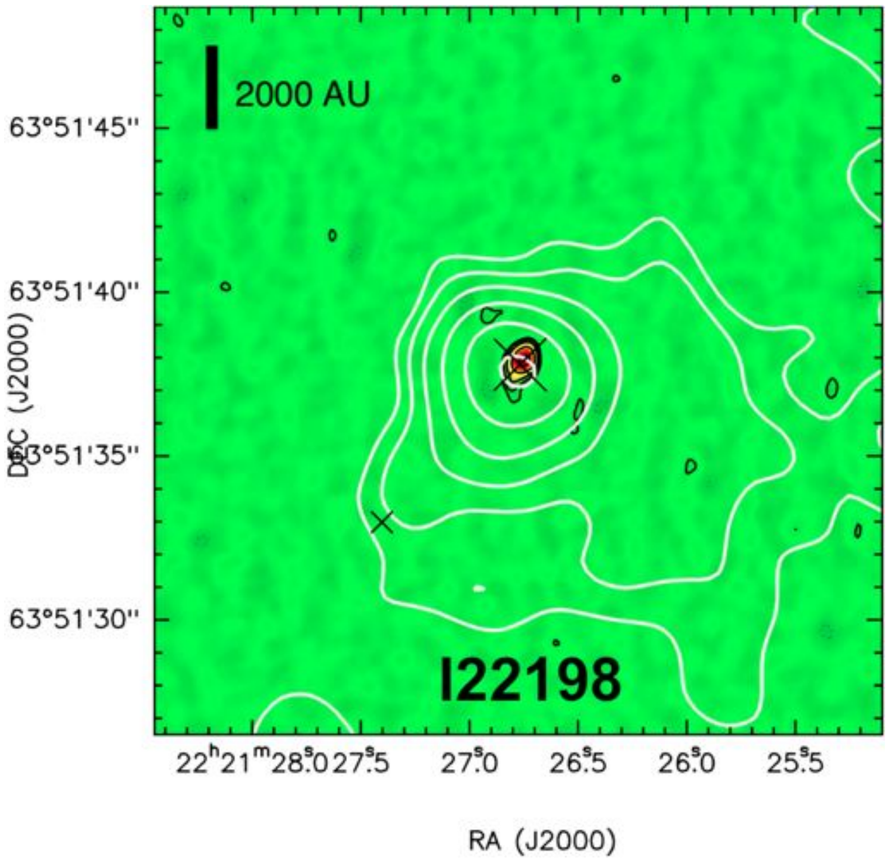

Spatial resolution: 300 AU
Mass sensitivity: 0.1 M_{sun}

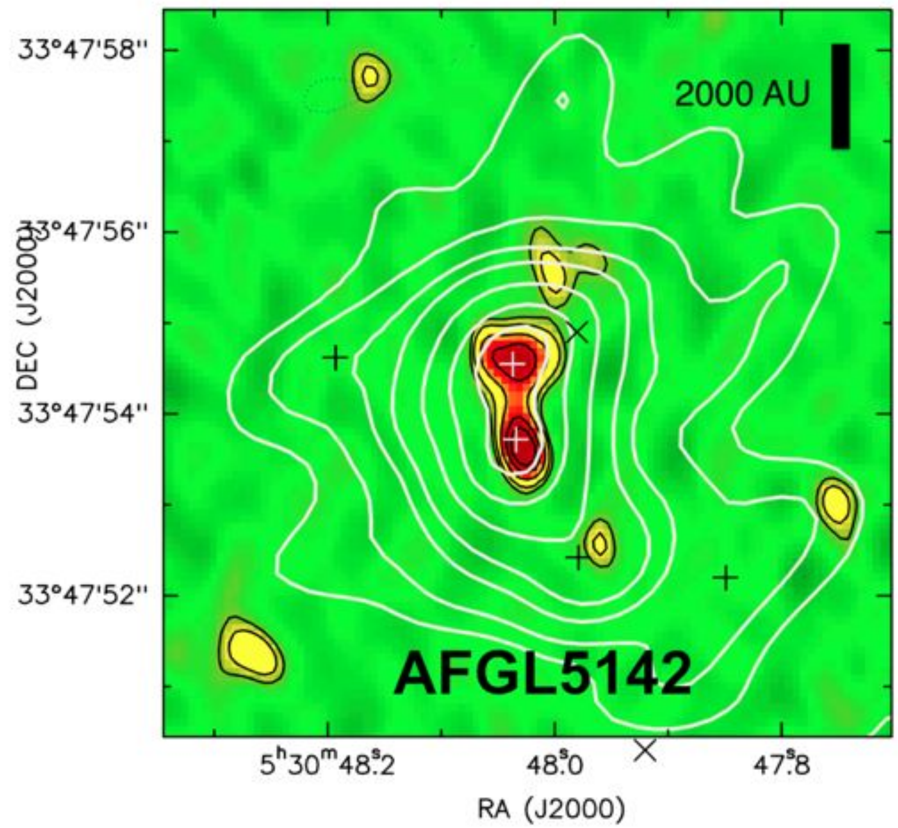

Spatial resolution: 700 AU
Mass sensitivity: 0.9 M_{sun}

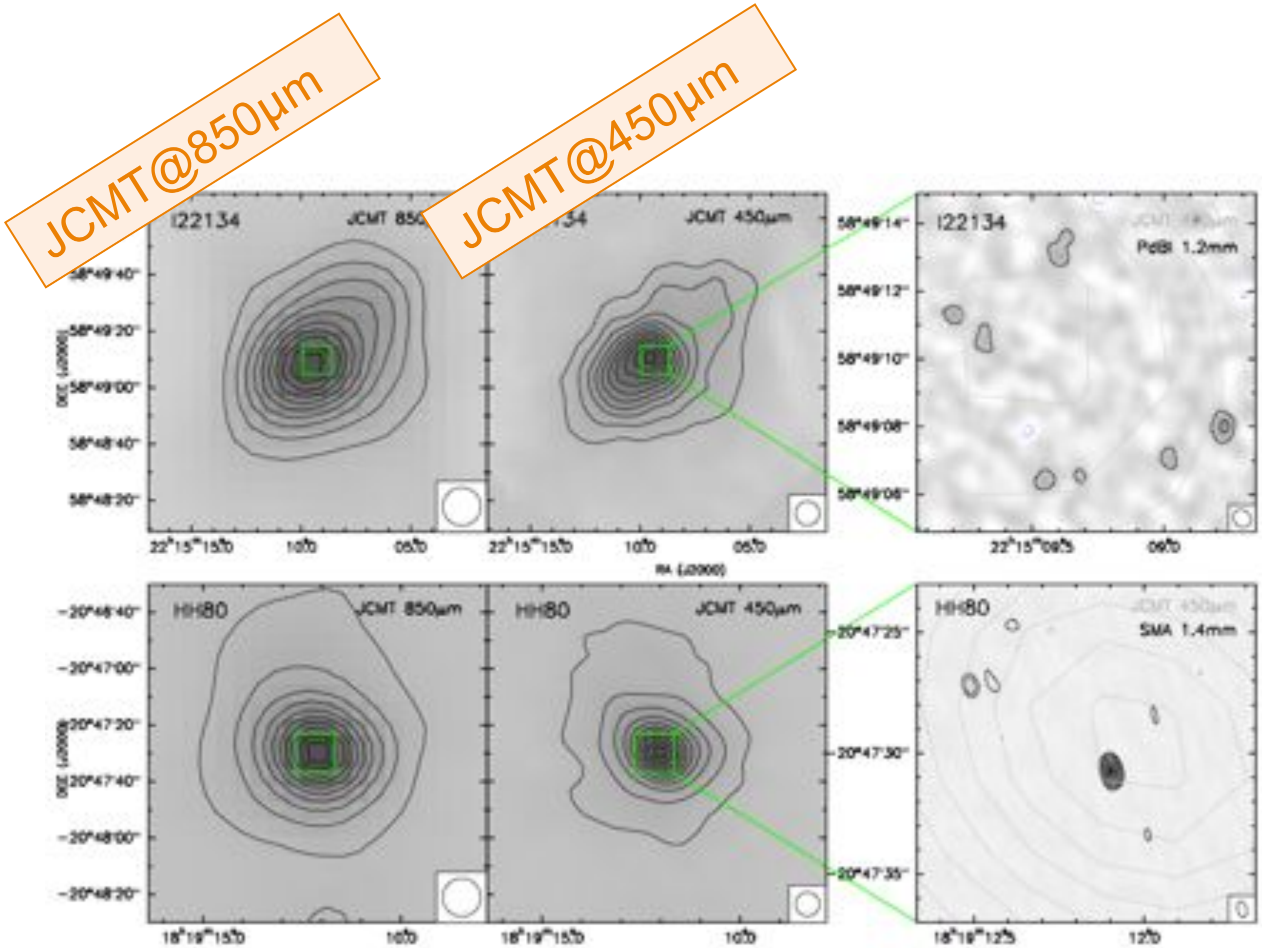

Using the mm/submm single-dish emission:

Flux

Half power contour

↓

Mass (T_d, opacity)

Avg surface density: $M/\pi R^2$

Avg density entire core: $3M/4\pi R^3$

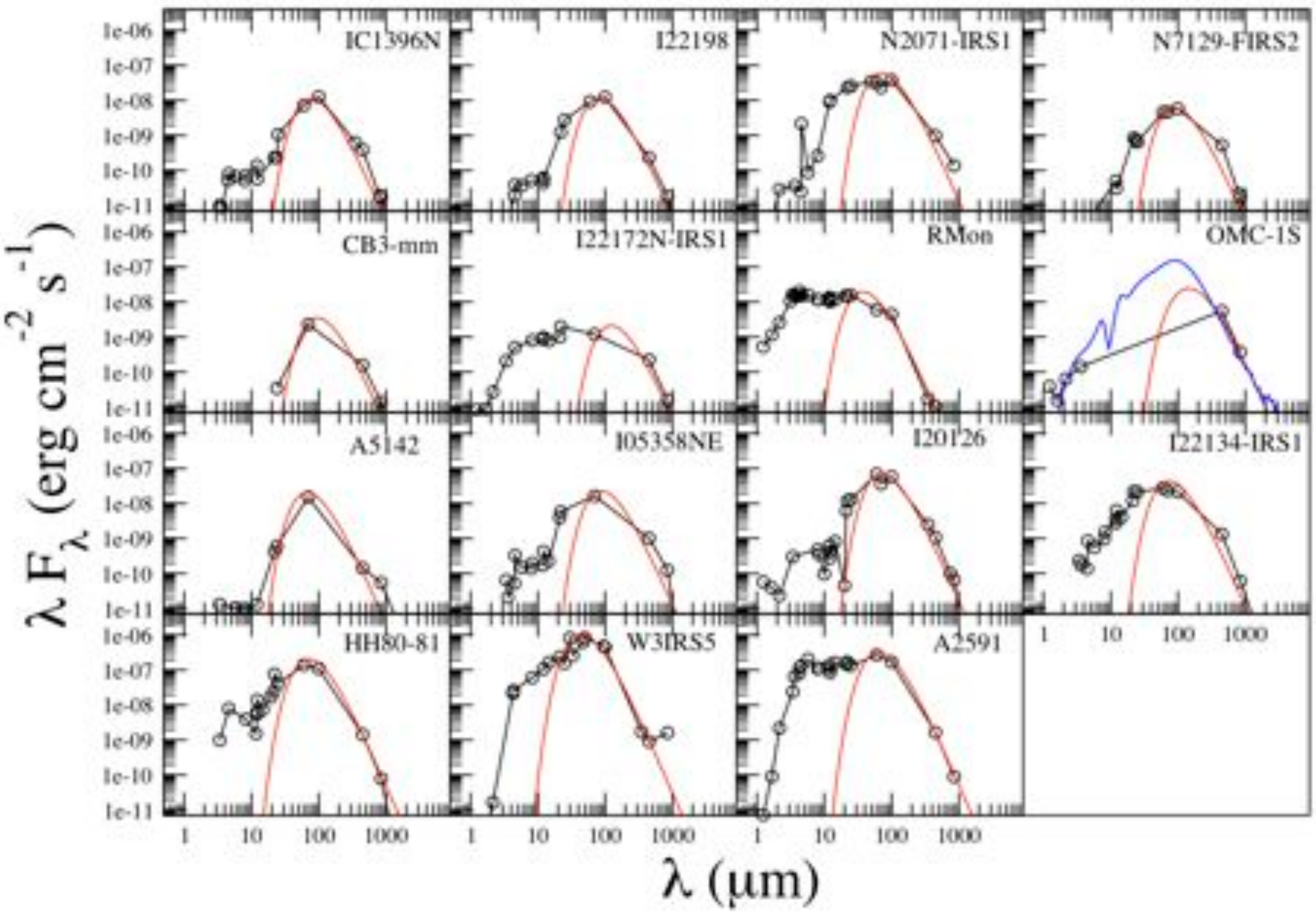

SEDs: IRAC,MIPS, MSX, IRAS, AKARI, SCUBA…

Calculate:

L_{bol} and L_{bol}/M_{sd}

In addition…

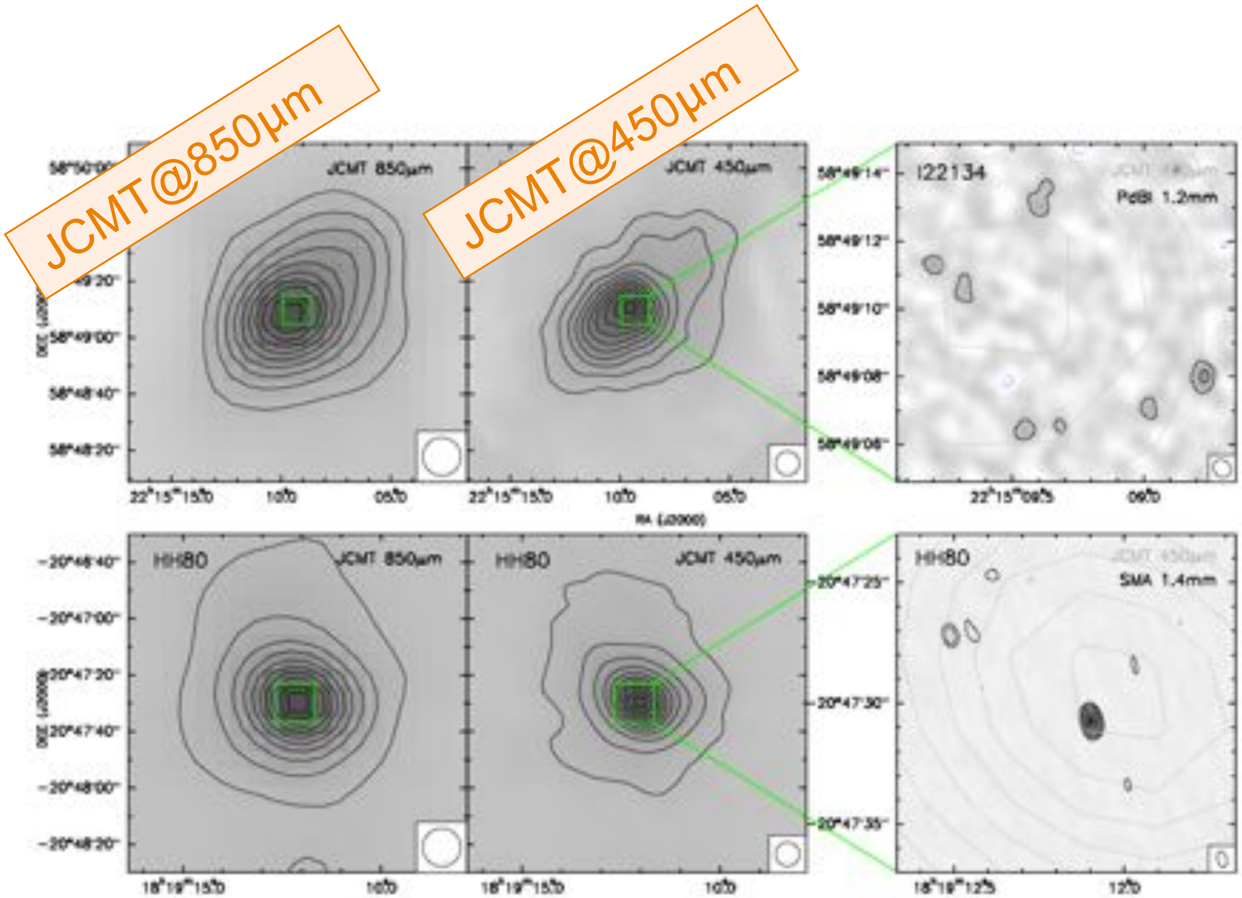

M_{max}: mass of strongest mm source measured by an interf in extended config.

Core Formation Efficiency:

$$CFE = \frac{\Sigma m_i}{M_{sd}}$$

Dependence of N_{mm} with L_{bol}, M_{sd}

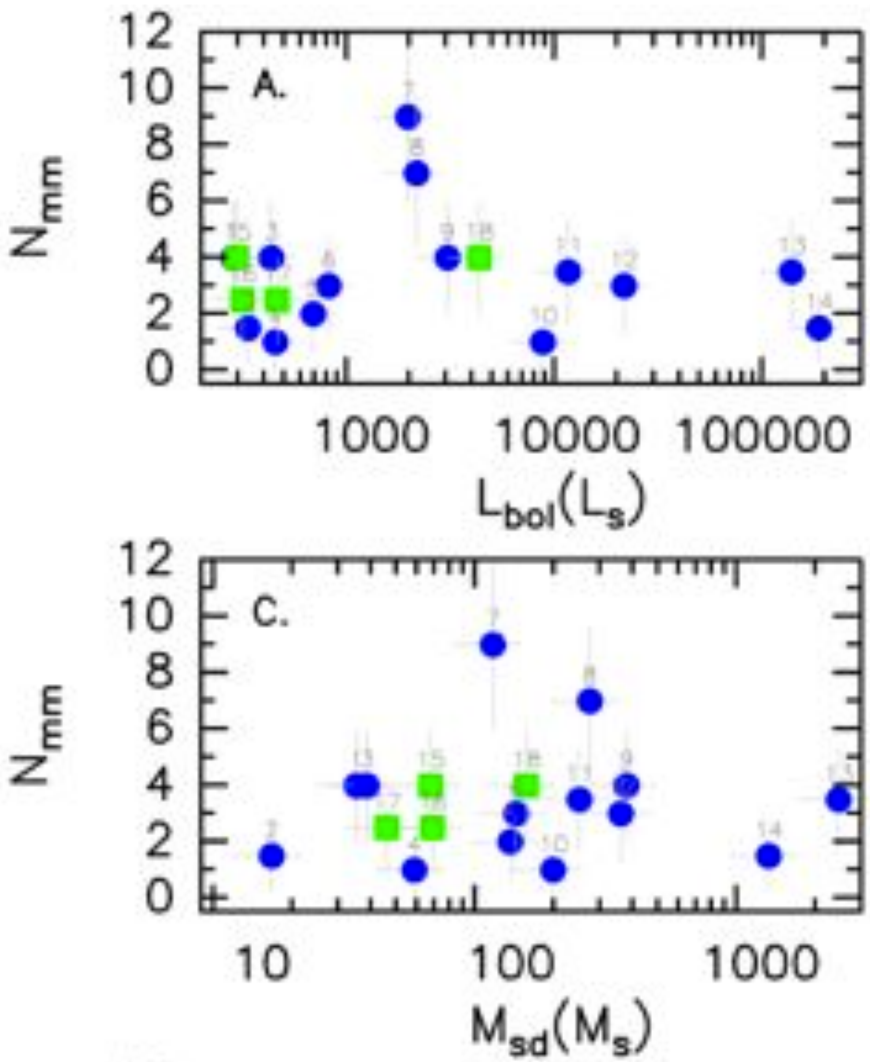

Dependence of N_{mm} with evolutionary stage and density of entire core, and CFE

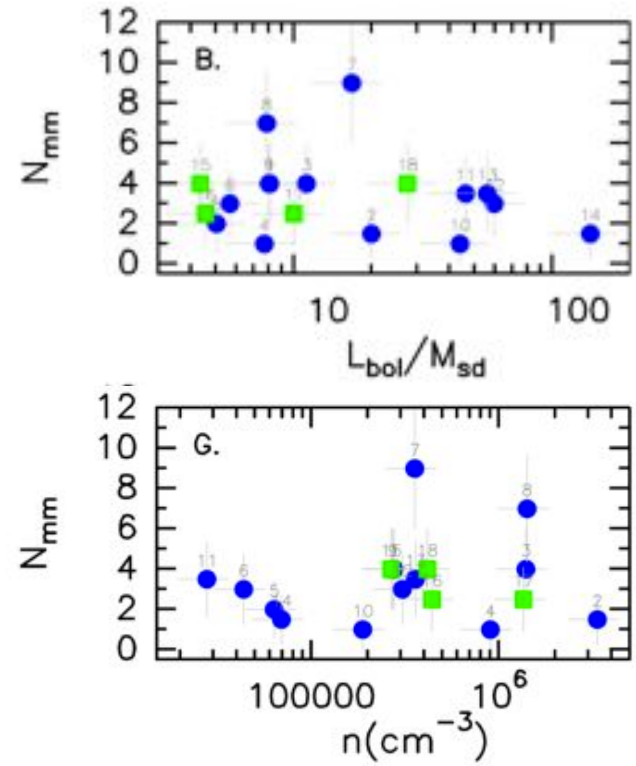

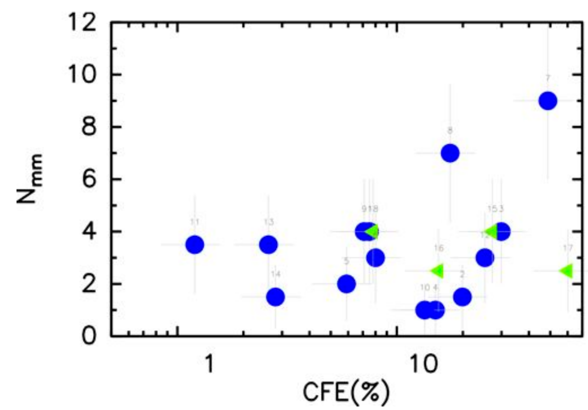

Palau et al. 2013, ApJ, 762, 120

Introduction

Method + First Results

One step forward: density and T

Role of turbulence and B

Model density and temperature structure of the dense cores

Assumptions:

- spherically symmetric envelope
- dust opacity $\kappa_\nu \propto \nu^\beta$
- density profile $\rho = \rho_0 \, (r/r_0)^{-p}$
- temperature profile $T = T_0 \, (r/r_0)^{-q}$, with $q = 2/(4+\beta)$
- external heating: T = 10 K in the outer envelope
- no assumption of optically thin emission
- no R-J approximation

First approximation (R-J, optically thin, no external heating):

power-law radial intensity profile, $I_\nu \propto b^{\,1-(p+q)}$

Meaningful comparison:

- convolution with beam (main+error model beams)
- chopping with 120" chop-throw (circularly averaged)

Fit simultaneously:

- intensity profiles at 850 and 450 μm
- SED from cm to 60 μm wavelengths (sensitive to T)

Model density and temperature profiles of the dense cores

Assumptions:

- spherically symmetric envelope
- dust opacity $\kappa_\nu \propto \nu^\beta$
- density profile $\rho = \rho_0 (r/r_0)^{-p}$
- temperature profile $T = T_0 (r/r_0)^{-q}$, with $q = 2/(4+\beta)$
- external heating: T = 10 K in the outer envelope
- no assumption of optically thin emission
- no R-J approximation

4 free parameters

~~**First approximation (R-J, optically thin, no external heating):**~~
~~power-law radial intensity profile, $I_\nu \propto b^{1-(p+q)}$~~

Meaningful comparison:

- convolution with beam (main+error model beams)
- chopping with 120" chop-throw (circularly averaged)

Fit simultaneously:

- intensity profiles at 850 and 450 μm
- SED from cm to 60 μm wavelengths (sensitive to T)

Model density and temperature profiles of the dense cores

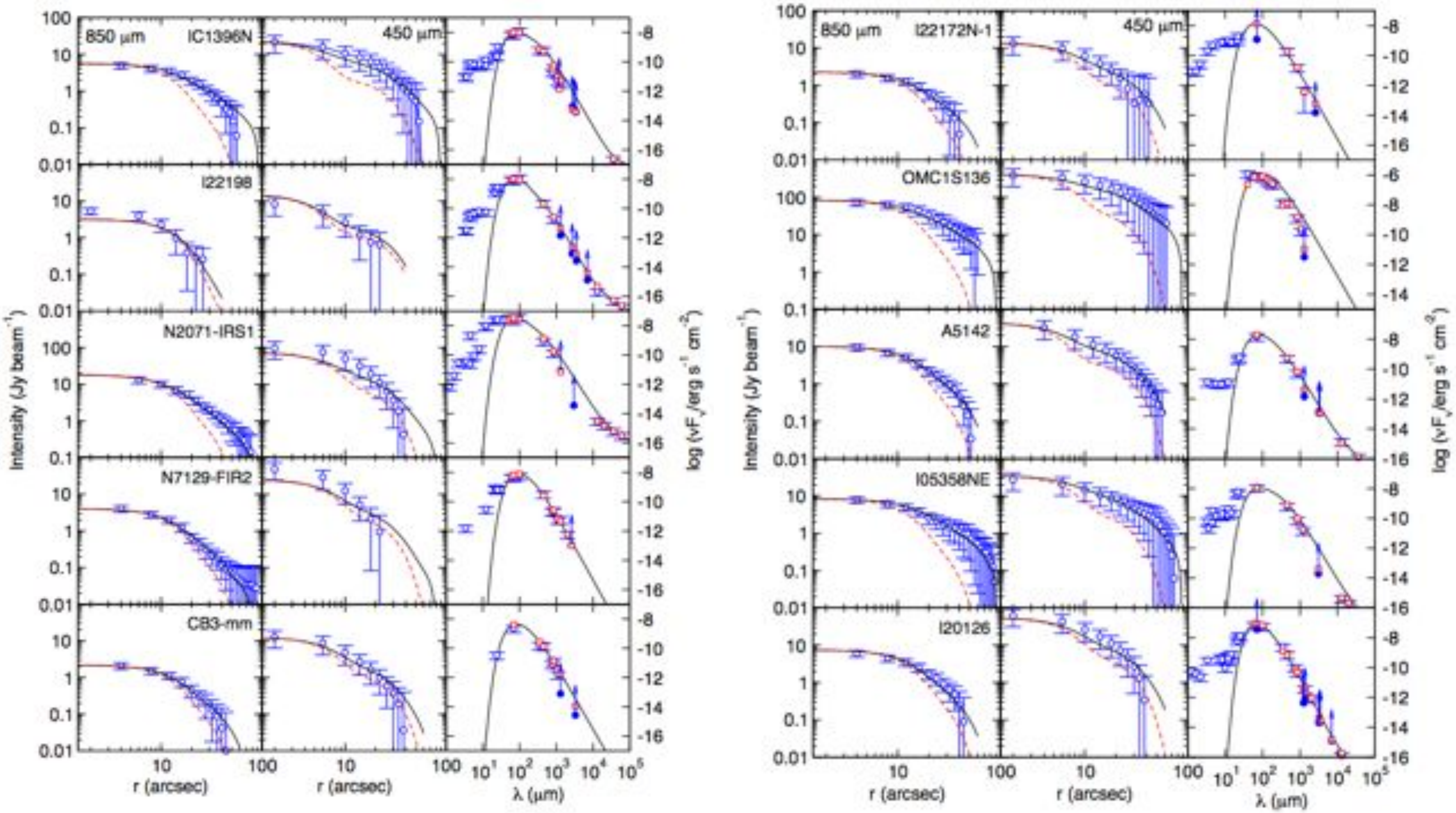

Palau et al. 2014, ApJ, 785, 42

Model density and temperature profiles of the dense cores

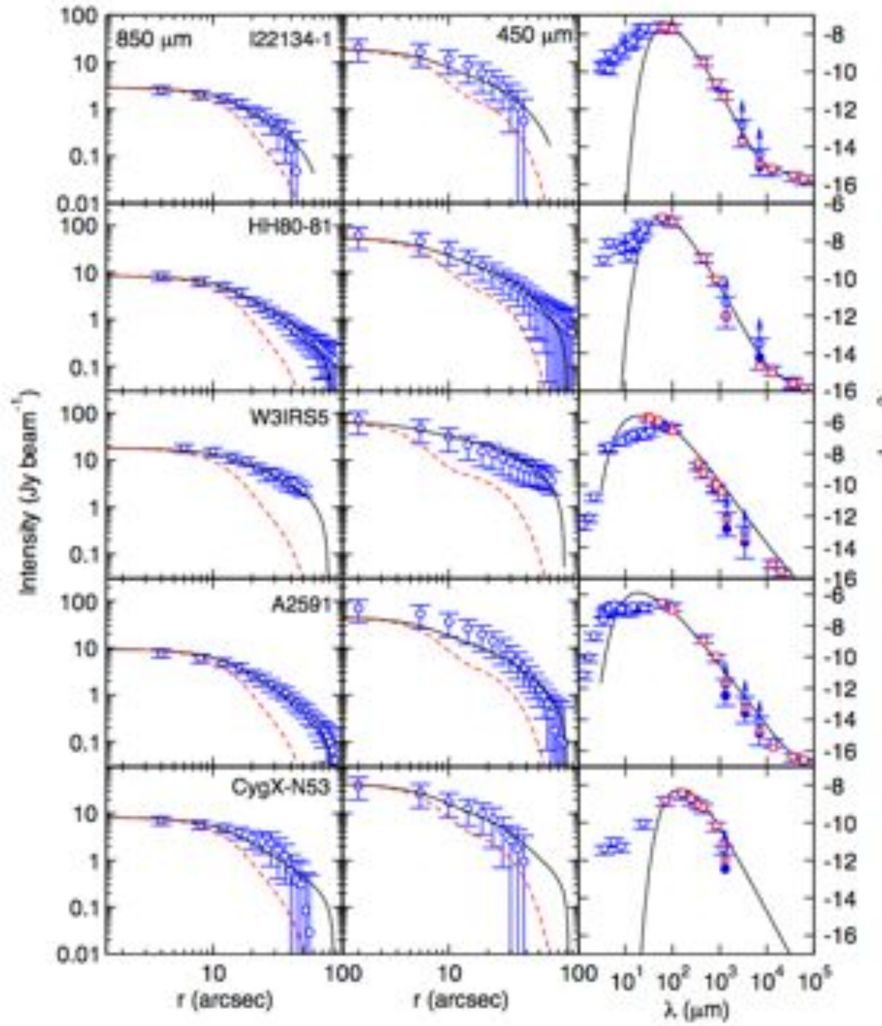

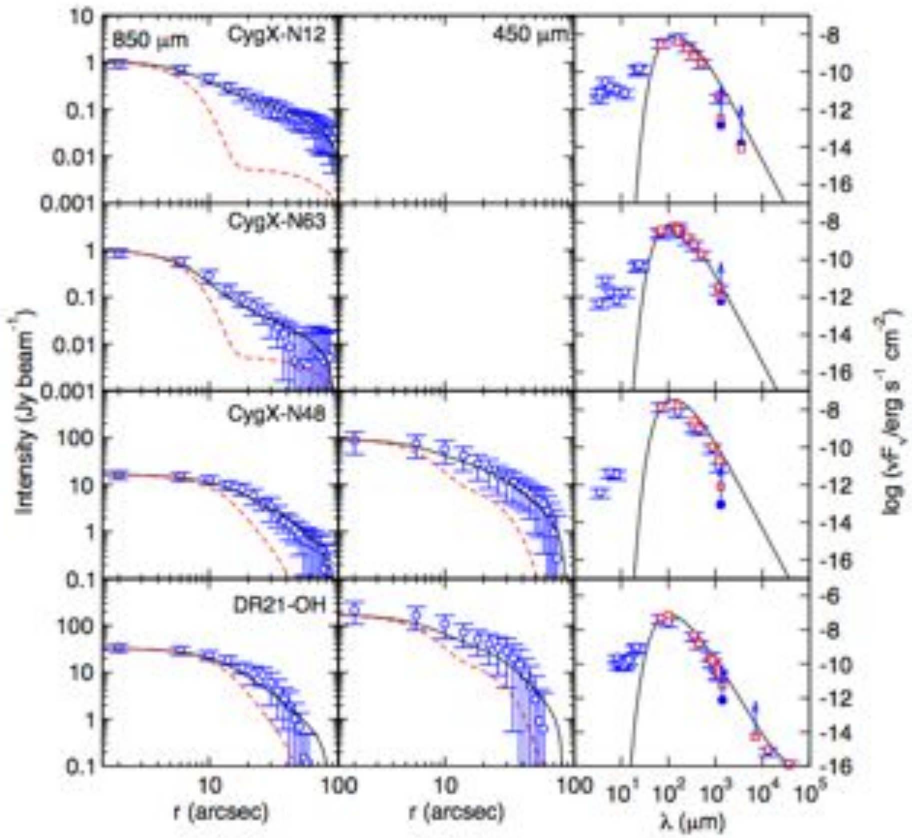

Palau et al. 2014, ApJ, 785, 42

Model density and temperature profiles of the dense cores

TABLE 1
BEST-FIT PARAMETERS TO THE RADIAL PROFILES AND SED OF THE MASSIVE DENSE CORES

ID-Source	D (kpc)	L_{bol} ($L_\odot$)	N_{mm}[a]	β[b]	T_0[b] (K)	ρ_0[b] (g cm^{-3})	p[b]	χ_r[b]	p_{lit}[c]	Refs.[c]
1-IC1396N[d]	0.75	290	4	1.41 ± 0.19	43 ± 4	$(2.8 \pm 0.4) \times 10^{-17}$	1.62 ± 0.08	0.580	1.2	1
2-I22198[e]	0.76	340	1.5	1.46 ± 0.31	43 ± 5	$(2.8 \pm 1.0) \times 10^{-17}$	2.45 ± 0.16	0.885	–	–
3-NGC2071-IRS1	0.42	440	4	1.09 ± 0.21	40 ± 3	$(6.1 \pm 1.0) \times 10^{-17}$	1.83 ± 0.09	0.534	–	–
4-NGC7129-FIRS2	1.25	460	1	1.55 ± 0.28	47 ± 4	$(5.9 \pm 1.1) \times 10^{-17}$	2.14 ± 0.11	0.454	1.4	1
5-CB3-mm	2.50	700	2	1.42 ± 0.24	58 ± 7	$(7.4 \pm 1.5) \times 10^{-17}$	2.04 ± 0.10	0.552	2.2	1
6-I22172N-IRS1	2.40	830	3	1.49 ± 0.23	75 ± 10	$(3.7 \pm 0.7) \times 10^{-17}$	1.89 ± 0.08	0.283	–	–
7-OMC-1S	0.45	2000	9	1.42 ± 0.20	86 ± 9	$(8.8 \pm 1.8) \times 10^{-17}$	1.56 ± 0.10	0.319	??	2
8-AFGL 5142[d]	1.80	2200	7	1.25 ± 0.20	70 ± 7	$(1.8 \pm 0.2) \times 10^{-16}$	2.00 ± 0.05	0.361	–	–
9-I05358+3543NE	1.80	3100	4	1.28 ± 0.18	62 ± 6	$(6.4 \pm 1.0) \times 10^{-17}$	1.55 ± 0.05	0.229	> 0.8,1.5	3,7
10-I20126+4104	1.64	8900	1	1.82 ± 0.24	86 ± 9	$(8.4 \pm 1.6) \times 10^{-17}$	2.21 ± 0.11	0.607	1.6,1.8,2.2	3,4,5
11-I22134-IRS1	2.60	11800	3.5	1.70 ± 0.19	82 ± 8	$(3.1 \pm 0.5) \times 10^{-17}$	1.76 ± 0.06	0.477	1.3	3
12-HH80-81	1.70	21900	3	1.56 ± 0.14	108 ± 10	$(4.2 \pm 0.6) \times 10^{-17}$	1.78 ± 0.04	0.473	–	–
13-W3IRS5[d]	1.95	140000	3.5	1.04 ± 0.12	260 ± 30	$(2.4 \pm 0.3) \times 10^{-17}$	1.46 ± 0.04	0.602	1.5,1.4	4,7
14-AFGL 2591	3.00	190000	1.5	0.96 ± 0.12	250 ± 20	$(5.4 \pm 0.7) \times 10^{-17}$	1.80 ± 0.03	0.549	1.0,2.0,1.0	4,6,7
15-CygX-N53	1.40	300	6?	1.55 ± 0.22	45 ± 4	$(9.7 \pm 1.8) \times 10^{-17}$	1.76 ± 0.07	0.487	–	–
16-CygX-N12[d]	1.40	320	2.5	1.75 ± 0.10	50 ± 7	$(3.3 \pm 1.0) \times 10^{-17}$	1.52 ± 0.10	0.376	–	–
17-CygX-N63[d]	1.40	470	1	1.80 ± 0.33	45 ± 3	$(6.5 \pm 1.1) \times 10^{-17}$	2.03 ± 0.07	0.570	–	–
18-CygX-N48	1.40	4400	5	1.88 ± 0.18	58 ± 5	$(1.0 \pm 1.7) \times 10^{-16}$	1.71 ± 0.05	0.459	–	–
19-DR21-OH	1.40	10000	11	1.60 ± 0.26	73 ± 7	$(3.1 \pm 0.6) \times 10^{-16}$	1.98 ± 0.08	0.808	1.8,1.4	4,7

Palau et al. 2014, ApJ, 785, 42

Dependence of N_{mm} with density power law index “p”

Dependence of N_{mm} with density at r=1000 AU

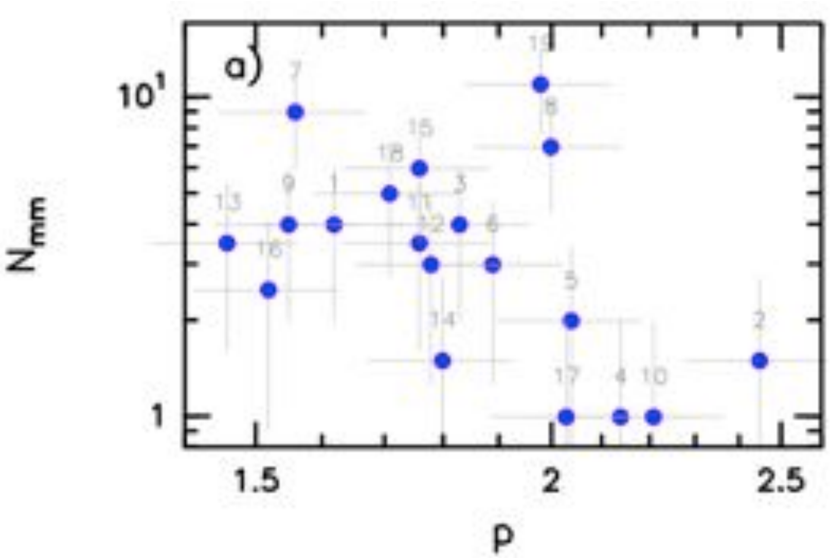

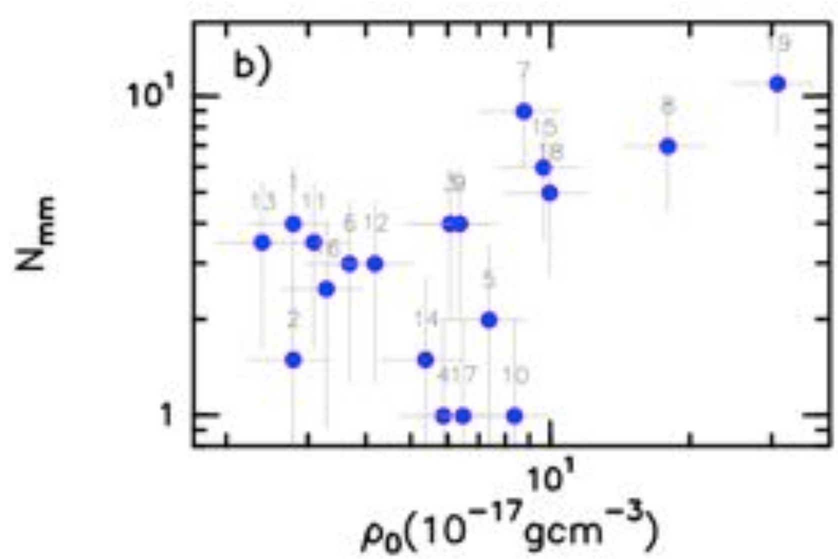

Palau et al. 2014, ApJ, 785, 42

Dependence of N_{mm} with density within diameter of 0.1 pc

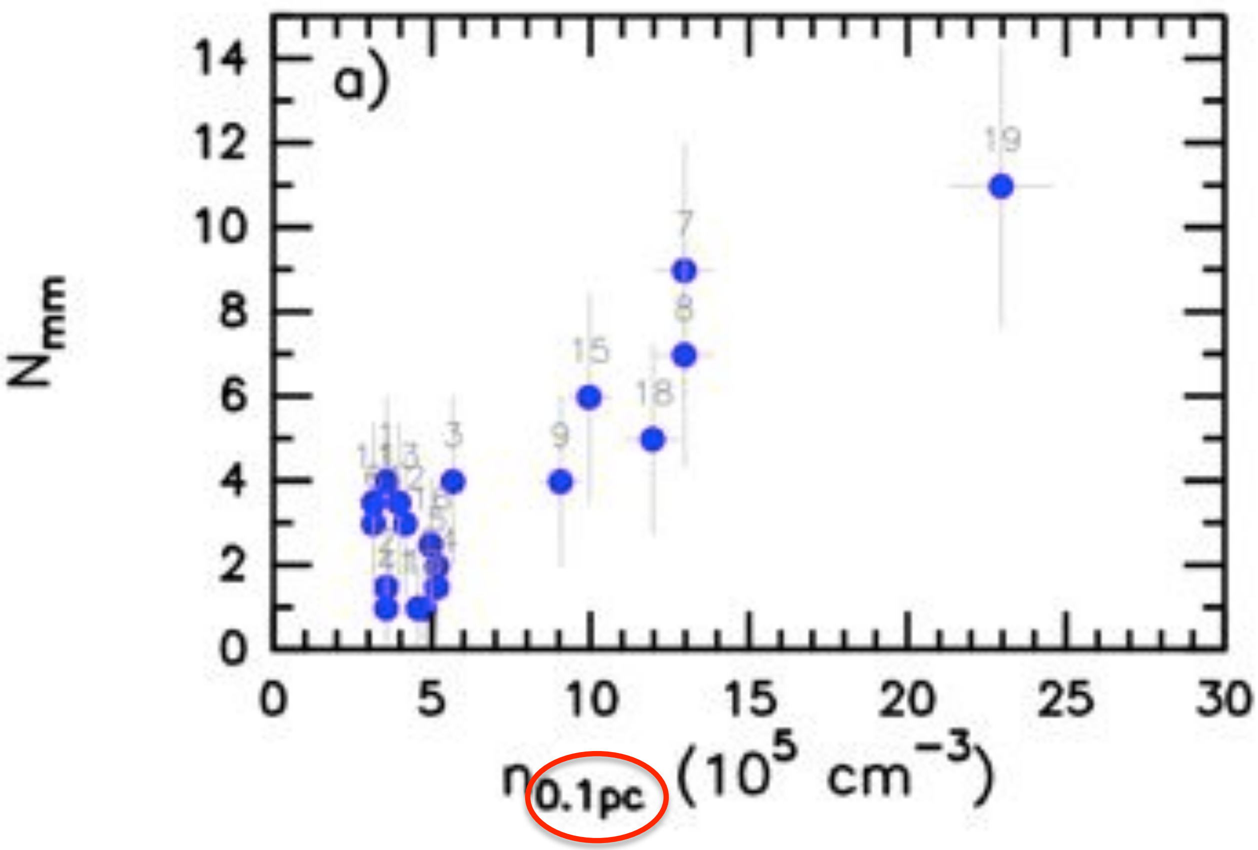

0.1 pc is the region where fragmentation (N_{mm}) was assessed!

Palau et al. 2014, ApJ, 785, 42

From the modeled n, T profiles: $M_{0.1pc}$ $n_{0.1pc}$ $T_{0.1pc}$

$$\left[\frac{M^{\rm th}_{\rm Jeans}}{M_\odot}\right] = 0.6285 \left[\frac{T}{10\,{\rm K}}\right]^{3/2} \left[\frac{n}{10^5\,{\rm cm}^{-3}}\right]^{-1/2}$$

Source	$N_{\rm mm}$	$M_{0.1pc}$ [a] ($M_\odot$)	$n_{0.1pc}$ [a] (10^5 cm^{-3})	$T_{0.1pc}$ [a] (K)	$\sigma^{\rm obs}_{\rm NH_3}$ [b] (km s^{-1})	$\sigma^{\rm nth}_{\rm NH_3}$ [b] (km s^{-1})	$\mathcal{M}_{\rm NH_3}$ [b]	$\sigma^{\rm obs}_{\rm N_2H^+}$ [b] (km s^{-1})	$\sigma^{\rm nth}_{\rm N_2H^+}$ [b] (km s^{-1})	$\mathcal{M}_{\rm N_2H^+}$ [b]
1-IC1396N	4	11	3.6	25	–	–	–	0.56	0.56	1.9
2-I22198[c]	1.5	11	3.6	26	0.47	0.44	1.4	–	–	–
3-N2071-1	4	17	5.7	24	0.72	0.72	2.5	–	–	–
4-N7129-2	1	11	3.6	35	–	–	–	0.51	0.50	1.4
5-CB3-mm	2	15	5.2	40	–	–	–	0.72	0.72	1.9
6-I22172N	3	9	3.2	48	0.59	0.58	1.4	0.87	0.86	2.1
7-OMC-1S	9	38	13	49	1.16	1.15	2.8	0.90	0.89	2.1
8-A5142	7	39	13	47	1.61	1.61	3.9	1.09	1.08	2.6
9-I05358NE	4	27	9.1	35	0.72	0.71	2.0	1.07	1.07	3.0
10-I20126	1	14	4.8	68	2.00	1.99	4.0	0.85	0.84	1.7
11-I22134	3.5	10	3.2	50	0.42	0.40	0.9	0.62	0.61	1.4
12-HH80-81	3	12	4.2	66	0.98	0.96	2.0	–	–	–
13-W3IRS5	3.5	12	4.0	138	2.17	2.15	3.1	1.18	1.17	1.7
14-A2591	1.5	16	5.2	147	1.57	1.55	2.1	–	–	–
15-Cyg-N53	6	30	10	27	0.42	0.41	1.3	0.76	0.76	2.4
16-Cyg-N12	2.5	15	5.0	29	–	–	–	0.89	0.89	2.8
17-Cyg-N63	1	14	4.6	31	–	–	–	0.72	0.72	2.2
18-Cyg-N48	5	35	12	36	1.06	1.06	3.0	1.28	1.28	3.6
19-DR21-OH	11	69	23	49	1.49	1.48	3.5	–	–	–

Palau, Ballesteros-Paredes, Vázquez-Semadeni et al. 2015, in prep.

According to global-hierarc.-chaotic gravit. contract. scenario:

$$\left[\frac{M_{\rm Jeans}^{\rm th}}{M_\odot}\right] = 0.6285\left[\frac{T}{10\,\rm K}\right]^{3/2}\left[\frac{n}{10^5\,\rm cm^{-3}}\right]^{-1/2}$$

T calculated from model (avg in 0.1pc)

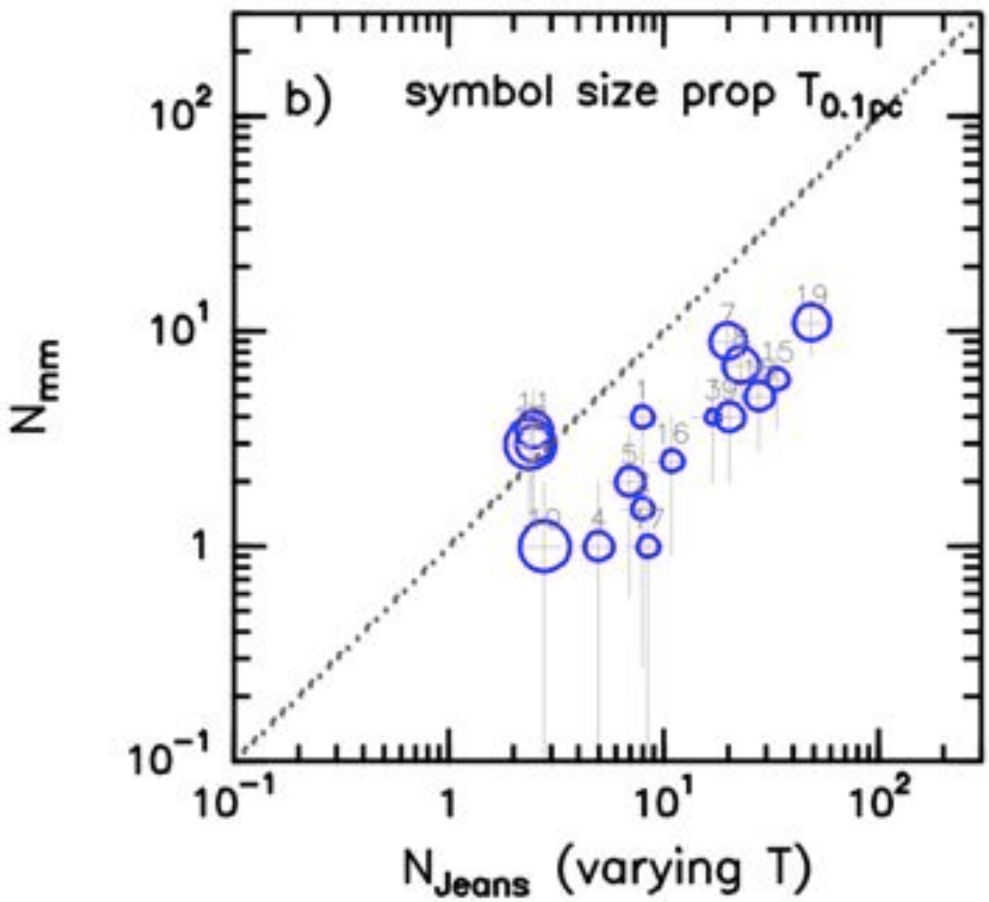

$$N_{\rm Jeans} = \frac{M_{0.1\rm pc}}{M_{\rm Jeans}}$$

Palau, Ballesteros-Paredes, Vázquez-Semadeni et al. 2015, in prep.

According to global-hierarc.-chaotic gravit. contract. scenario:

$$\left[\frac{M_{\rm Jeans}^{\rm th}}{M_\odot}\right] = 0.6285 \left[\frac{T}{10\,{\rm K}}\right]^{3/2} \left[\frac{n}{10^5\,{\rm cm}^{-3}}\right]^{-1/2}$$

T calculated from model (avg in 0.1pc)

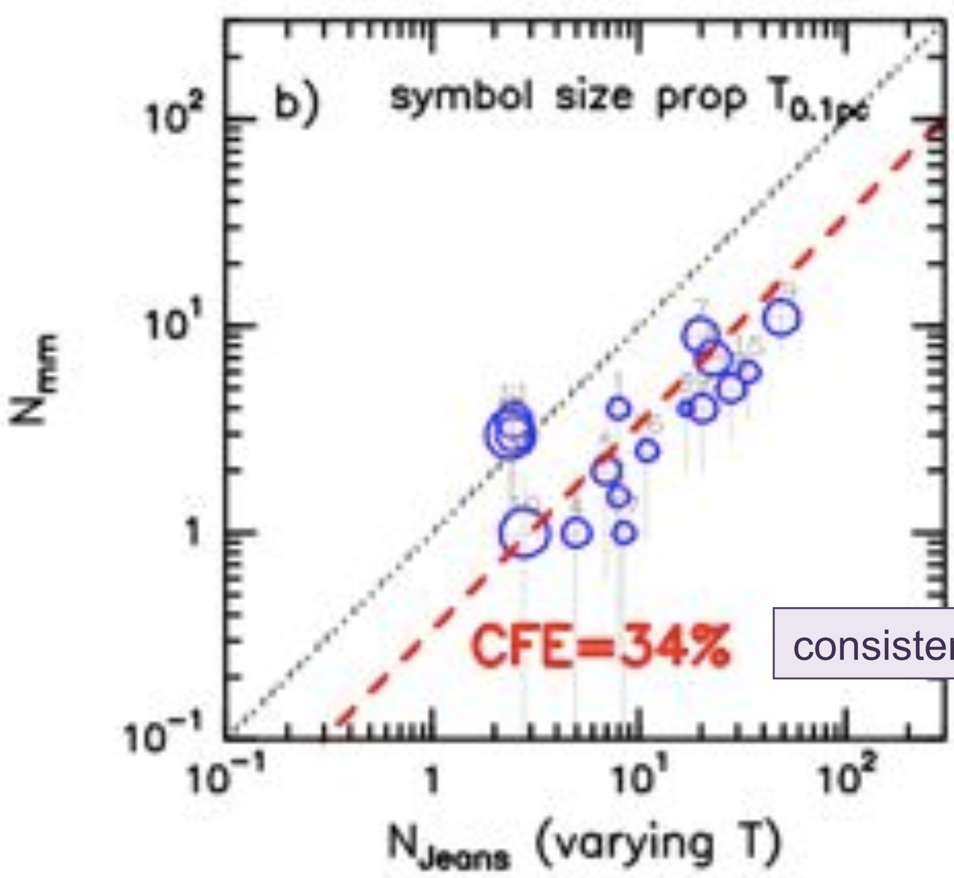

$$N_{\rm Jeans} = \frac{M_{0.1\rm pc}\,{\rm CFE}}{M_{\rm Jeans}}$$

consistent with Louvet+14 for n~10^5 cm^{-3}

Palau, Ballesteros-Paredes, Vázquez-Semadeni et al. 2015, in prep.

Introduction

Method + First Results

One step forward: density and T

Role of turbulence and B

What about turbulence?

VLA, USA
Archive + Sánchez-Monge, Palau et al. 2013, MNRAS + literature

IRAM30m, Spain
Fontani, Palau et al. 2011 + literature

NH_3(1,1): VLA, beam~5'', largest angular scale ~30''
N_2H^+(1—0): IRAM30m, beam~26''

NH3(1,1) emission with the VLA

Study the kinematics of the massive dense cores

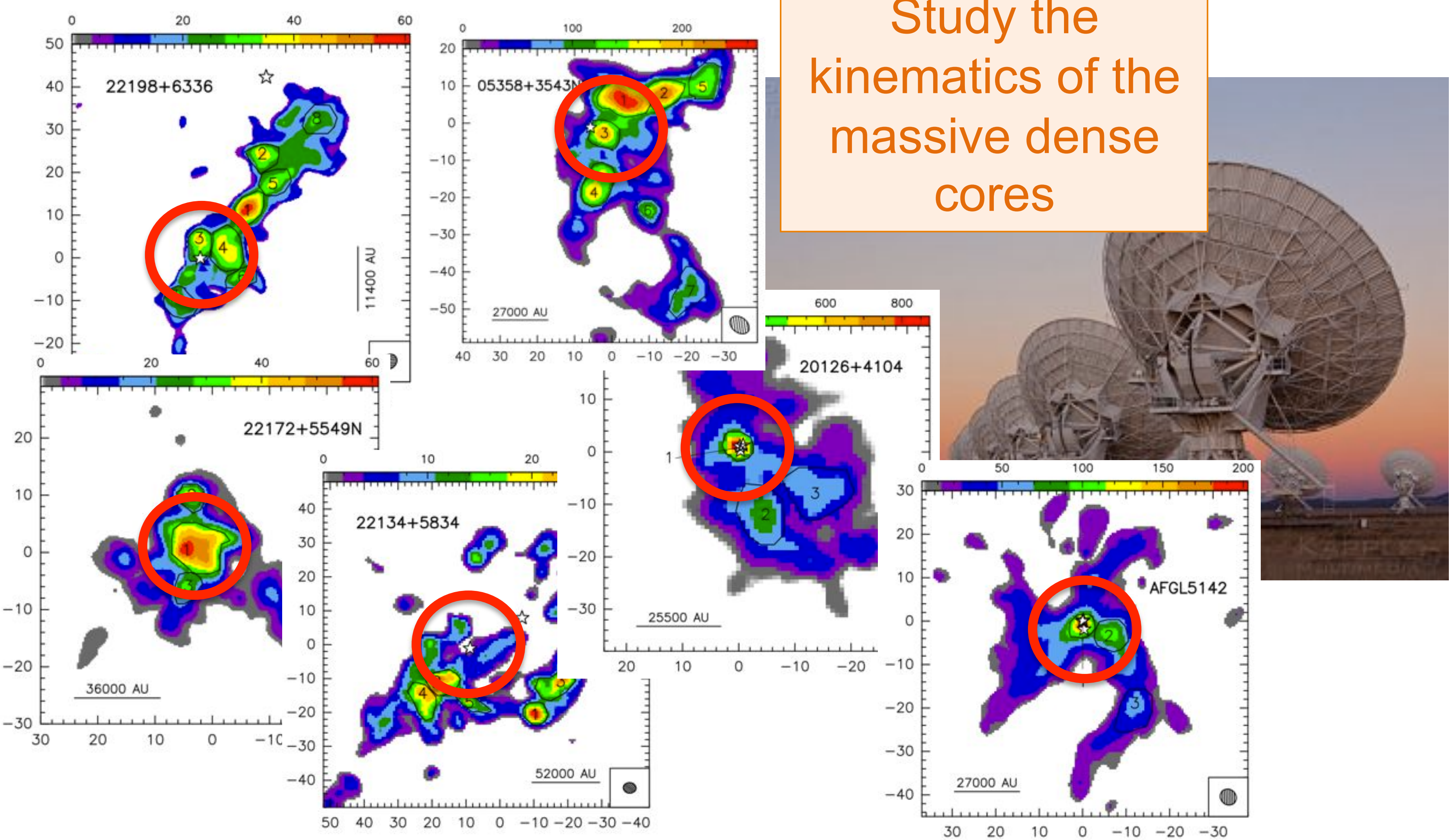

Sánchez-Monge, Palau et al. 2013, MNRAS, 432, 3288

NH3(1,1) emission with the VLA

Moment 2 maps:

$\sigma_{no\text{-}th}$: non-thermal velocity dispersion

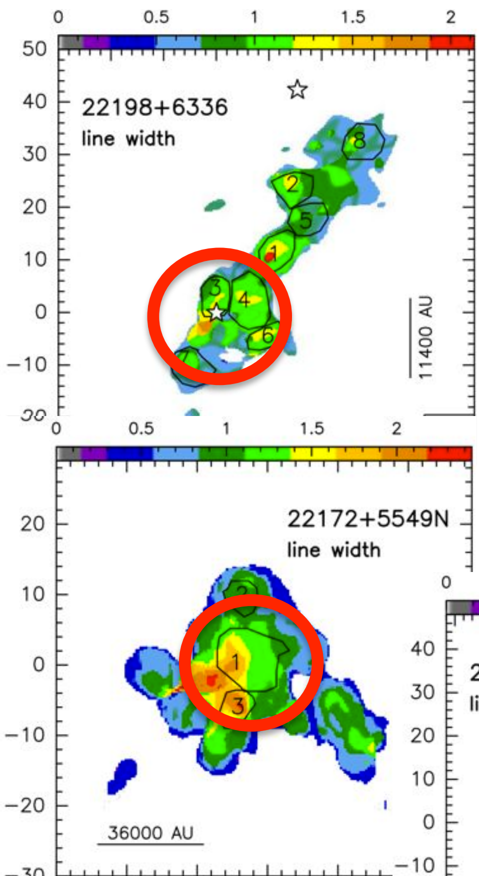

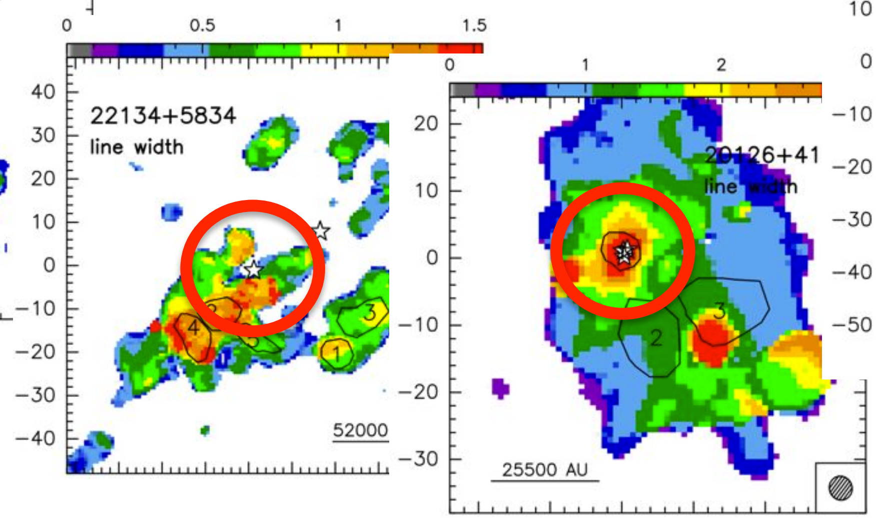

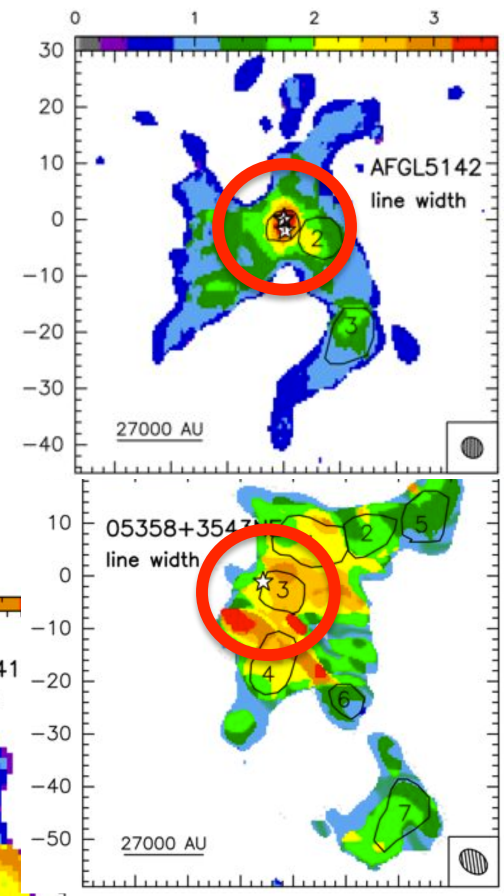

From the modeled temperature profile... estimate non-thermal contribution

Table 1. Modeled

Source	N_{mm}	$M_{0.1pc}$[a] ($M_\odot$)	$n_{0.1pc}$[a] (10^5 cm^{-3})	$T_{0.1pc}$[a] (K)	$\sigma^{obs}_{NH_3}$[b] (km s^{-1})	$\sigma^{nth}_{NH_3}$[b] (km s^{-1})	$\mathcal{M}_{NH_3}$[b]	$\sigma^{obs}_{N_2H^+}$[b] (km s^{-1})	$\sigma^{nth}_{N_2H^+}$[b] (km s^{-1})	$\mathcal{M}_{N_2H^+}$[b]
1-IC1396N	4	11	3.6	25	–	–	–	0.56	0.56	1.9
2-I22198[c]	1.5	11	3.6	26	0.47	0.44	1.4	–	–	–
3-N2071-1	4	17	5.7	24	0.72	0.72	2.5	–	–	–
4-N7129-2	1	11	3.6	35	–	–	–	0.51	0.50	1.4
5-CB3-mm	2	15	5.2	40	–	–	–	0.72	0.72	1.9
6-I22172N	3	9	3.2	48	0.59	0.58	1.4	0.87	0.86	2.1
7-OMC-1S	9	38	13	49	1.16	1.15	2.8	0.90	0.89	2.1
8-A5142	7	39	13	47	1.61	1.61	3.9	1.09	1.08	2.6
9-I05358NE	4	27	9.1	35	0.72	0.71	2.0	1.07	1.07	3.0
10-I20126	1	14	4.8	68	2.00	1.99	4.0	0.85	0.84	1.7
11-I22134	3.5	10	3.2	50	0.42	0.40	0.9	0.62	0.61	1.4
12-HH80-81	3	12	4.2	66	0.98	0.96	2.0	–	–	–
13-W3IRS5	3.5	12	4.0	138	2.17	2.15	3.1	1.18	1.17	1.7
14-A2591	1.5	16	5.2	147	1.57	1.55	2.1	–	–	–
15-Cyg-N53	6	30	10	27	0.42	0.41	1.3	0.76	0.76	2.4
16-Cyg-N12	2.5	15	5.0	29	–	–	–	0.89	0.89	2.8
17-Cyg-N63	1	14	4.6	31	–	–	–	0.72	0.72	2.2
18-Cyg-N48	5	35	12	36	1.06	1.06	3.0	1.28	1.28	3.6
19-DR21-OH	11	69	23	49	1.49	1.48	3.5	–	–	–

$NH_3(1,1)$ $N_2H^+(1—0)$

Palau, Ballesteros-Paredes, Vázquez-Semadeni et al. 2015, in prep.

Relation of N_{mm} with non-thermal vel. dispersion

Correl coeff: 0.26

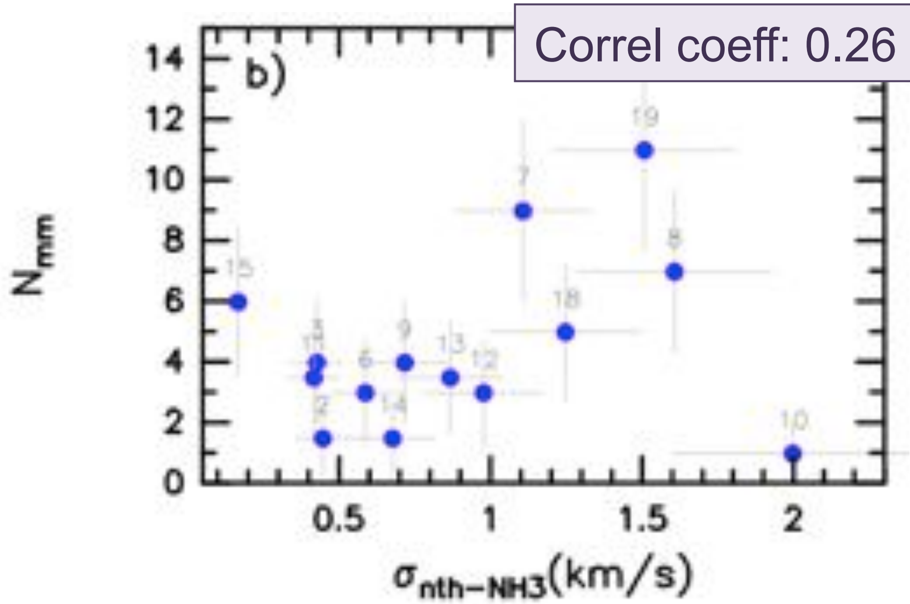

Correl coeff: 0.39

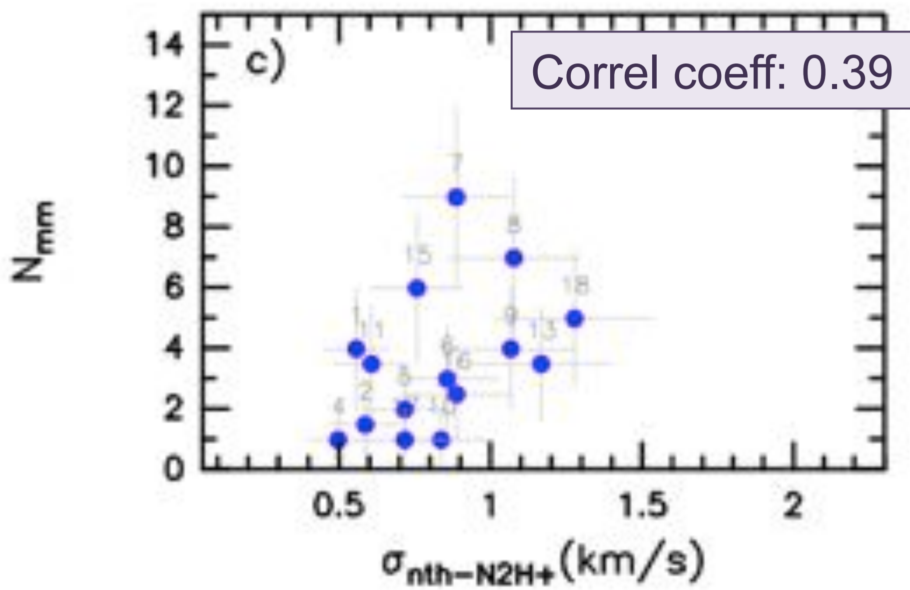

Reminder:

Correl coeff: 0.89

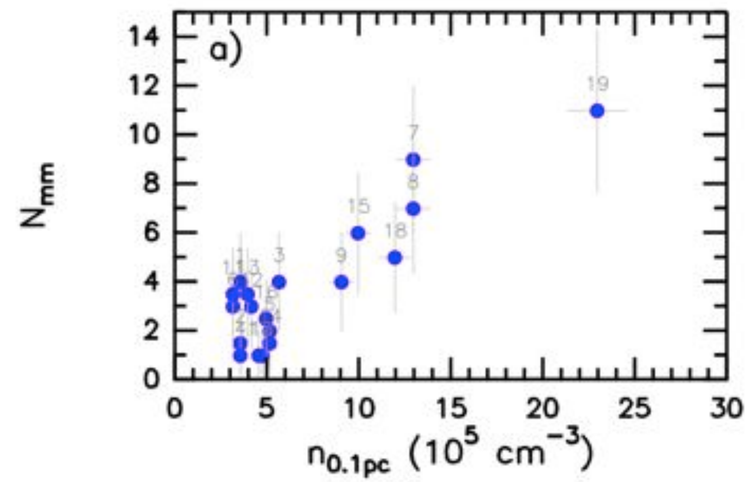

Palau, Ballesteros-Paredes, Vázquez-Semadeni et al. 2015, in prep.

$$N_{\rm Jeans} = \frac{M_{0.1\rm pc}\,{\rm CFE}}{M_{\rm Jeans}}$$

assuming CFE=100%

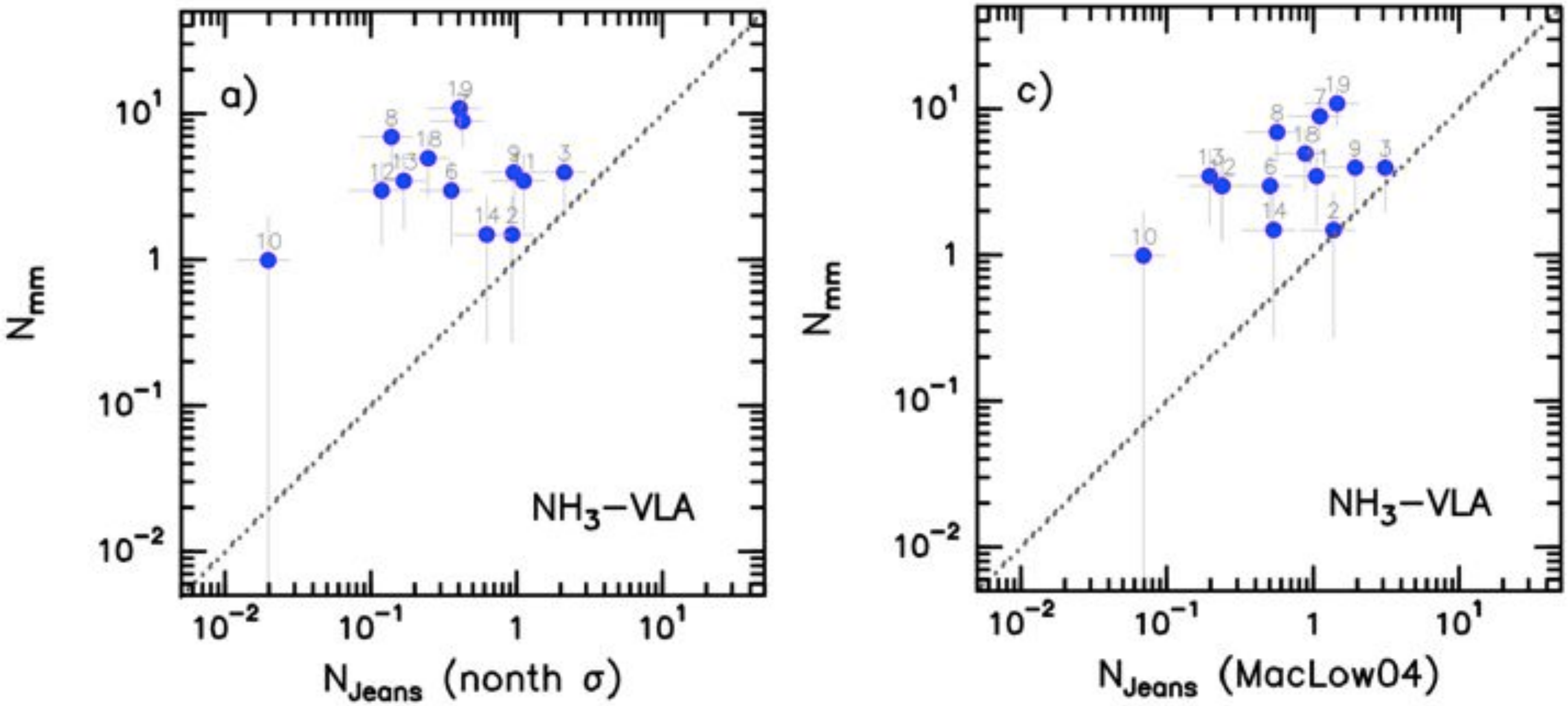

$$\left[\frac{M_{\rm Jeans}^{\rm nth}}{M_\odot}\right] = 1.578\left[\frac{\sigma_{\rm nth}}{0.188\,{\rm km\,s^{-1}}}\right]^3\left[\frac{n}{10^5\,{\rm cm^{-3}}}\right]^{-1/2}$$

$$\left[\frac{M_{\rm Jeans}^{\rm conv.flows}}{M_\odot}\right] = 1.578\left[\frac{\sigma_{\rm nth}}{0.188\,{\rm km\,s^{-1}}}\right]^3\left[\frac{n\,\mathcal{M}^2}{10^5\,{\rm cm^{-3}}}\right]^{-1/2}$$

According to turbulence-regulated quasi-equilibrium scenario:

Palau, Ballesteros-Paredes, Vázquez-Semadeni et al. 2015, in prep.

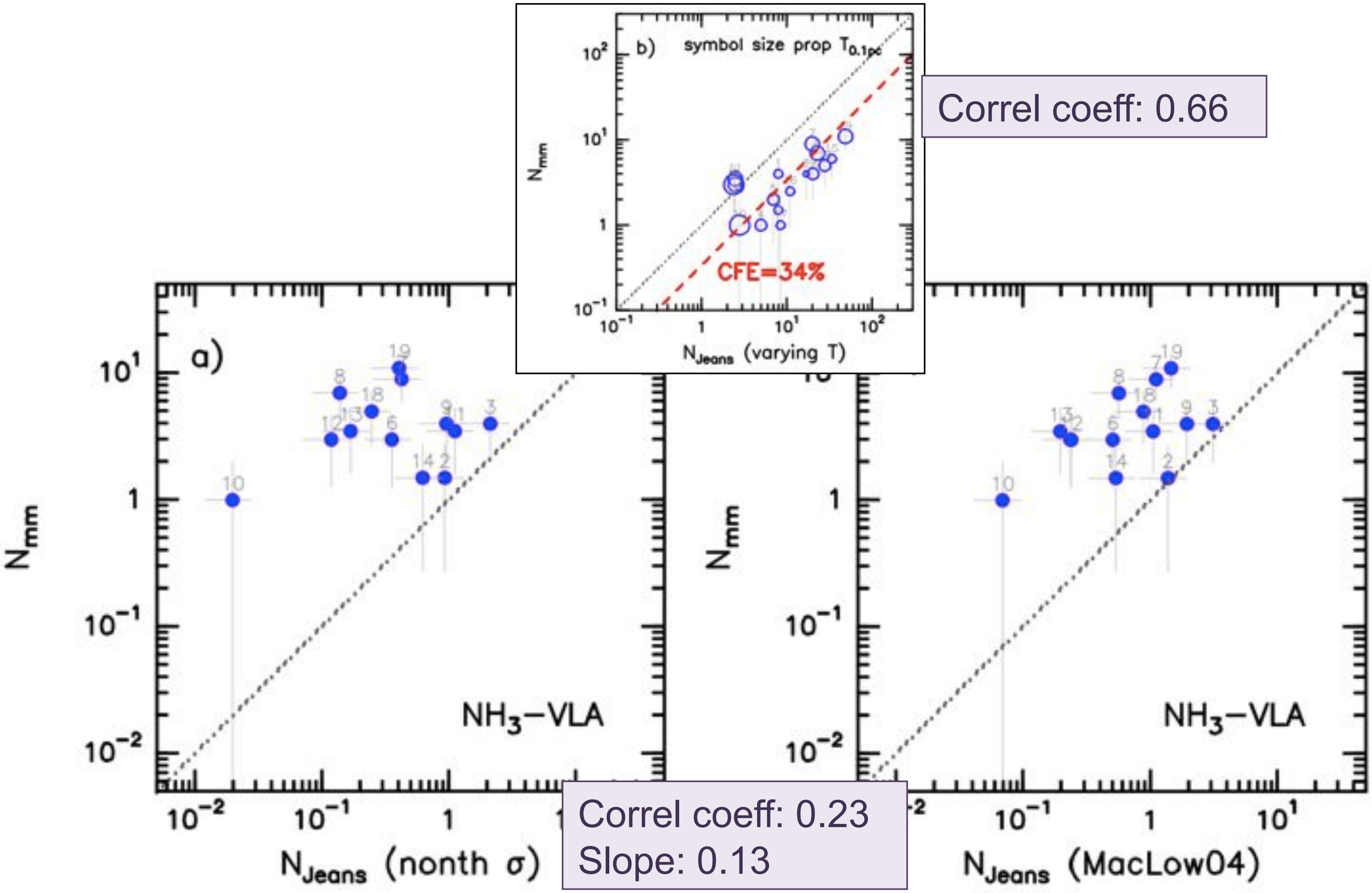

Correl coeff: 0.66

Correl coeff: 0.23
Slope: 0.13

$$\left[\frac{M_{\rm Jeans}^{\rm nth}}{M_\odot}\right] = 1.578 \left[\frac{\sigma_{\rm nth}}{0.188\,{\rm km\,s^{-1}}}\right]^3 \left[\frac{n}{10^5\,{\rm cm^{-3}}}\right]^{-1/2}$$

$$\left[\frac{M_{\rm Jeans}^{\rm conv.flows}}{M_\odot}\right] = 1.578 \left[\frac{\sigma_{\rm nth}}{0.188\,{\rm km\,s^{-1}}}\right]^3 \left[\frac{n\,\mathcal{M}^2}{10^5\,{\rm cm^{-3}}}\right]^{-1/2}$$

According to turbulence-regulated quasi-equilibrium scenario:

Palau, Ballesteros-Paredes, Vázquez-Semadeni et al. 2015, in prep.

$$N_{\rm Jeans} = \frac{M_{0.1\rm pc}\,{\rm CFE}}{M_{\rm Jeans}}$$

assuming CFE=100%

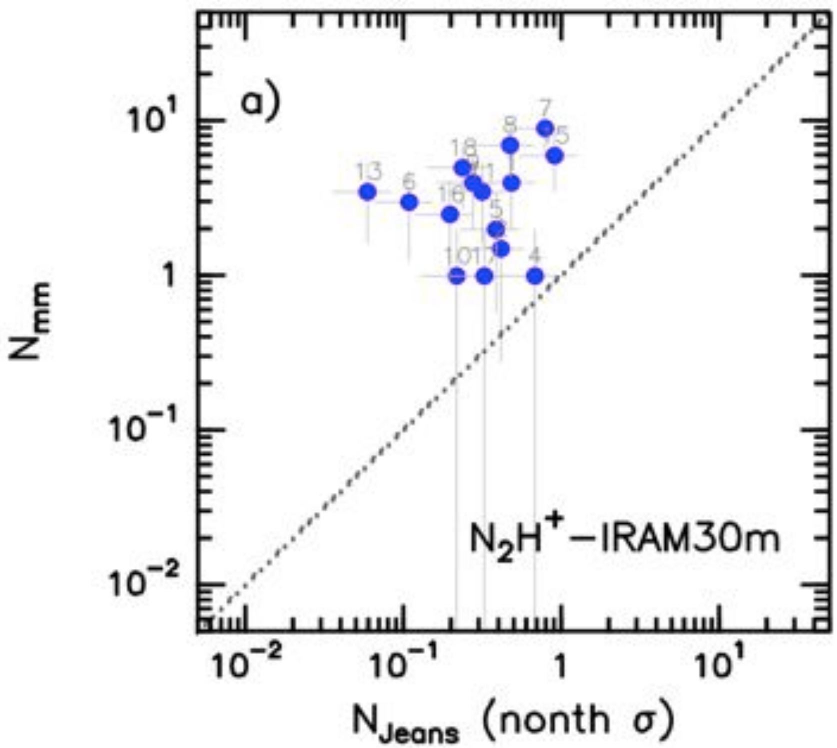

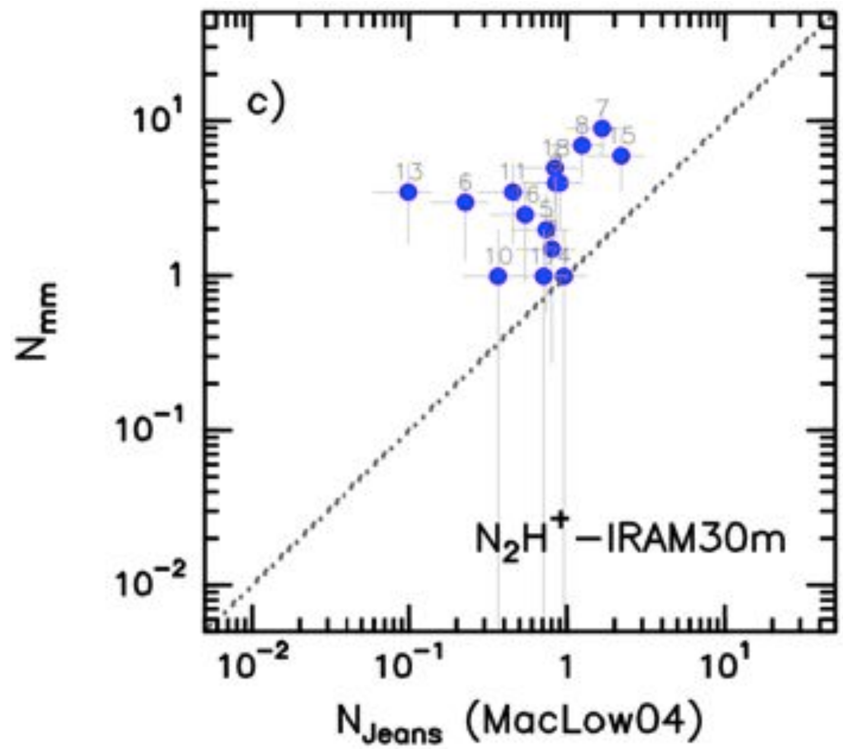

$$\left[\frac{M_{\rm Jeans}^{\rm nth}}{M_\odot}\right] = 1.578\left[\frac{\sigma_{\rm nth}}{0.188\,{\rm km\,s^{-1}}}\right]^3\left[\frac{n}{10^5\,{\rm cm^{-3}}}\right]^{-1/2}$$

$$\left[\frac{M_{\rm Jeans}^{\rm conv.flows}}{M_\odot}\right] = 1.578\left[\frac{\sigma_{\rm nth}}{0.188\,{\rm km\,s^{-1}}}\right]^3\left[\frac{n\,\mathcal{M}^2}{10^5\,{\rm cm^{-3}}}\right]^{-1/2}$$

According to turbulence-regulated quasi-equilibrium scenario:

Palau, Ballesteros-Paredes, Vázquez-Semadeni et al. 2015, in prep.

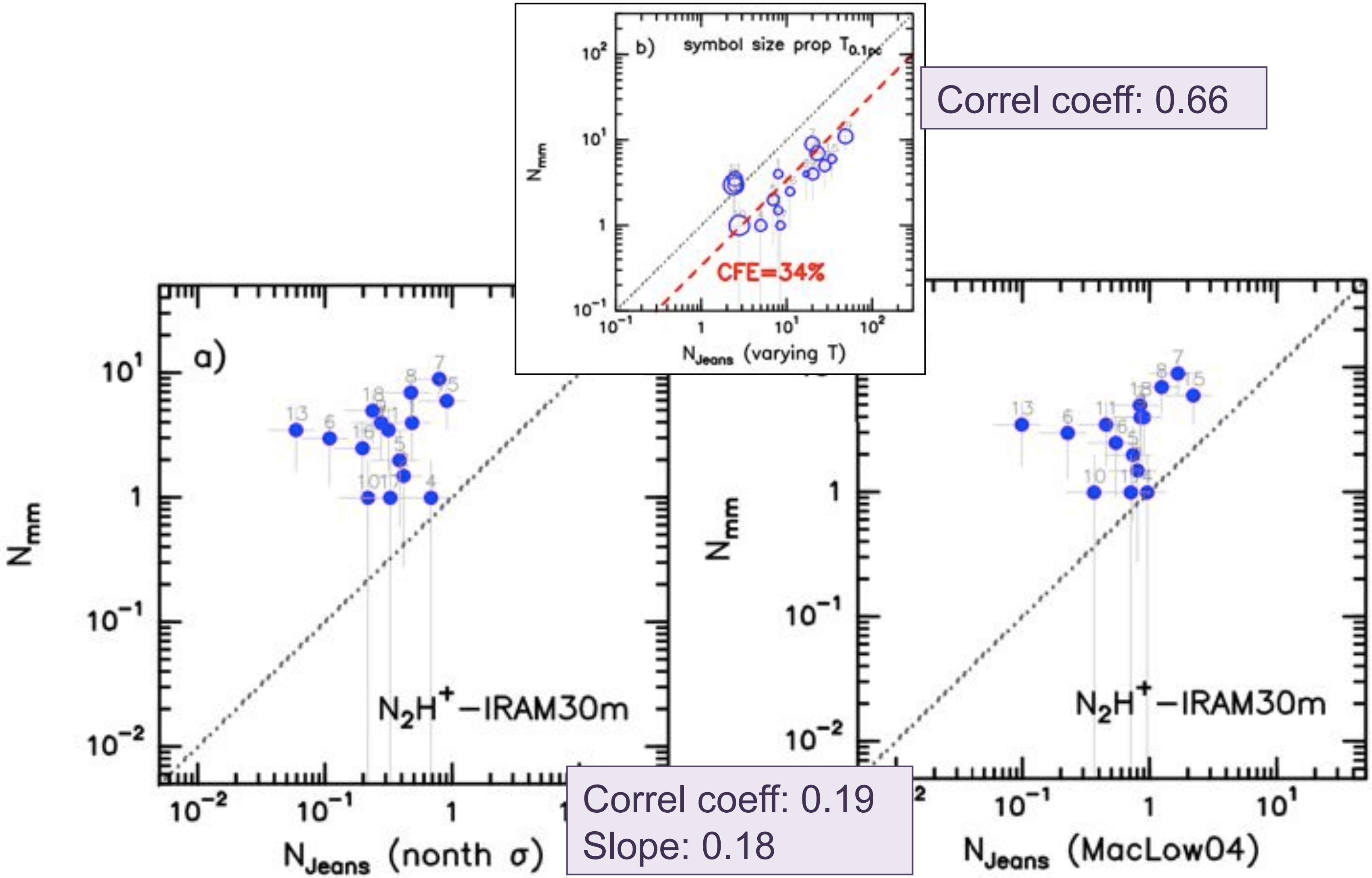

Correl coeff: 0.66

Correl coeff: 0.19
Slope: 0.18

$$\left[\frac{M_{\rm Jeans}^{\rm nth}}{M_\odot}\right] = 1.578\left[\frac{\sigma_{\rm nth}}{0.188\,{\rm km\,s^{-1}}}\right]^3\left[\frac{n}{10^5\,{\rm cm^{-3}}}\right]^{-1/2}$$

$$\left[\frac{M_{\rm Jeans}^{\rm conv.flows}}{M_\odot}\right] = 1.578\left[\frac{\sigma_{\rm nth}}{0.188\,{\rm km\,s^{-1}}}\right]^3\left[\frac{n\,\mathcal{M}^2}{10^5\,{\rm cm^{-3}}}\right]^{-1/2}$$

According to turbulence-regulated quasi-equilibrium scenario:

Palau, Ballesteros-Paredes, Vázquez-Semadeni et al. 2015, in prep.

Our data are better described by pure thermal support. This means that:

1) either we are not properly measuring the turbulence level of dense cores

2) or turb cannot be treated as an additional pressure term to thermal pressure (ie, M_{Jeans} should be described in a different way)

3) or turbulence does not have a crucial role in determining the fragmentation level of dense cores

What about magnetic field?

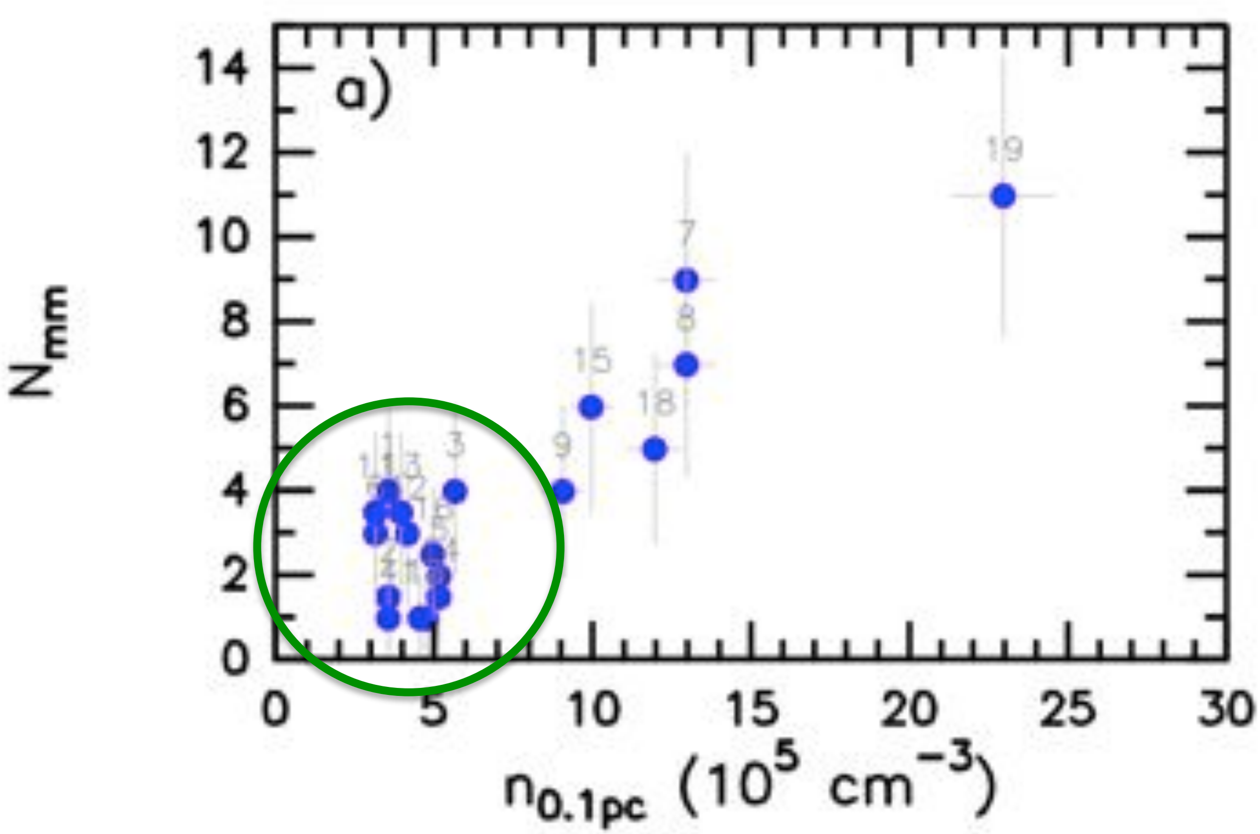

B knwon to suppress fragmentation:

How would simulations including different B compare in this plot?

Magnetohydrodynamical simulations including radiation transport:

Commerçon et al. 2011, after Hennebelle et al. 2011

Strongly magnetized core

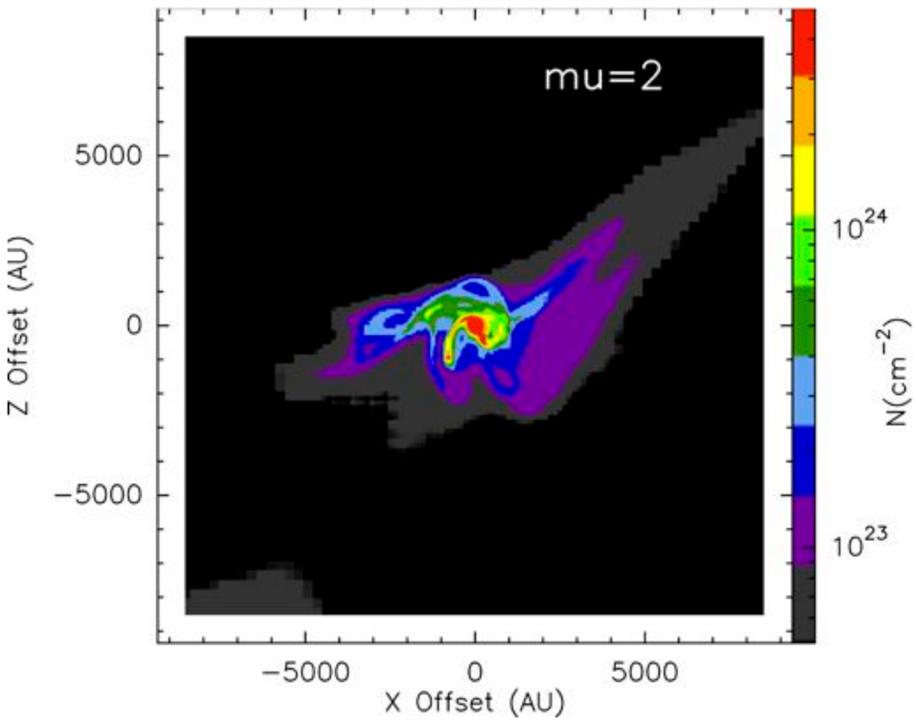

Weakly magnetized core

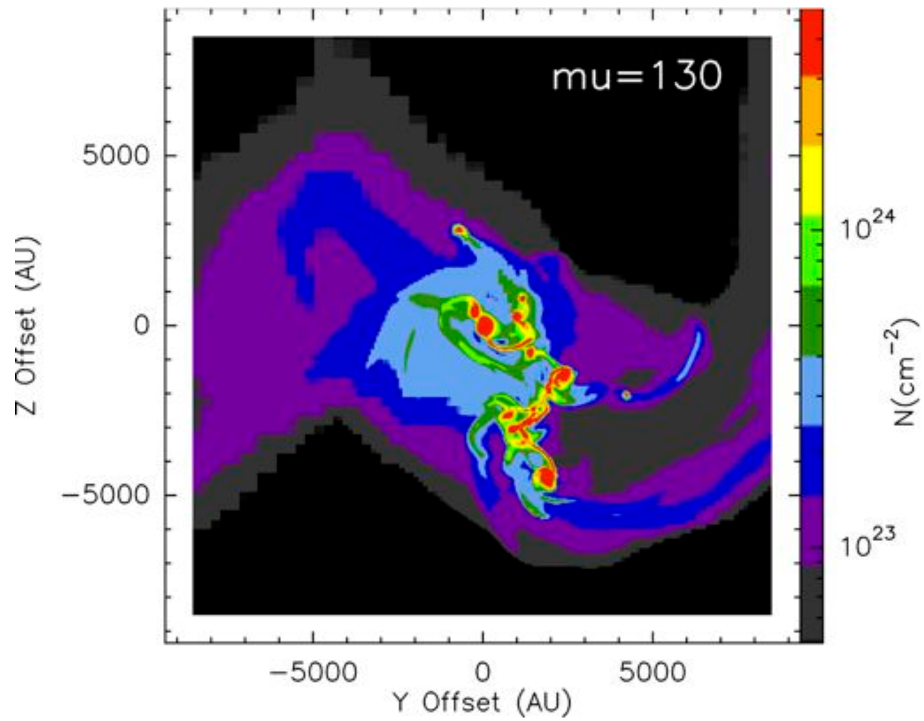

Compare fragmentation level

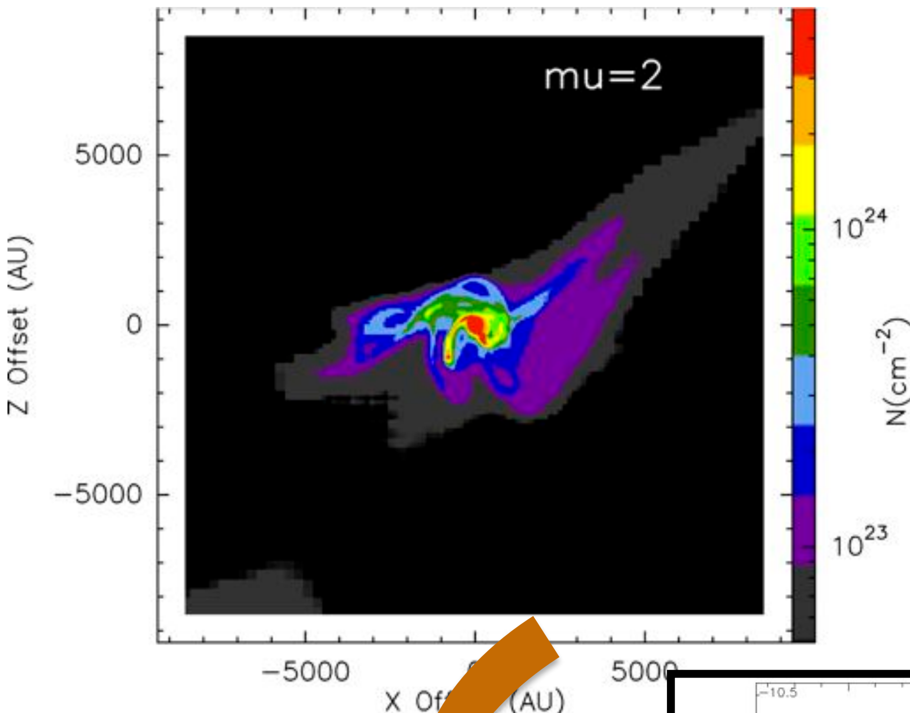

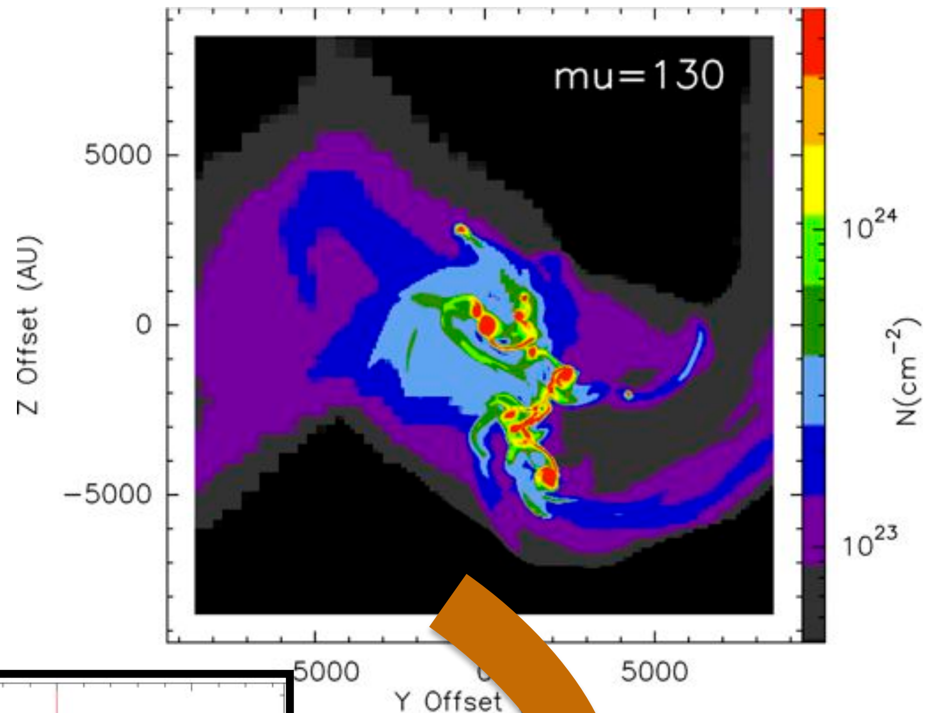

Convolution with Plateau de Bure A *uv*-coverage

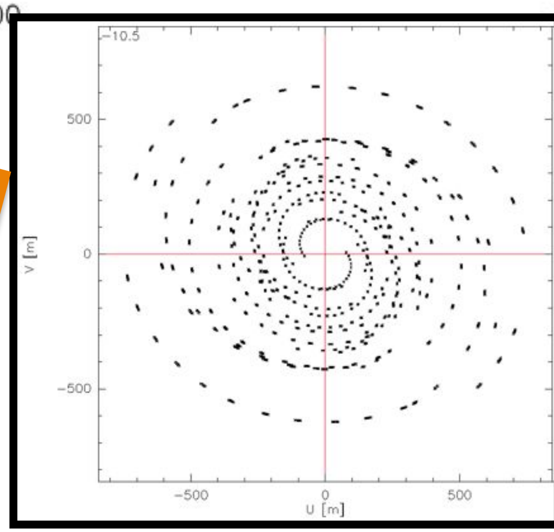

Compare fragmentation level

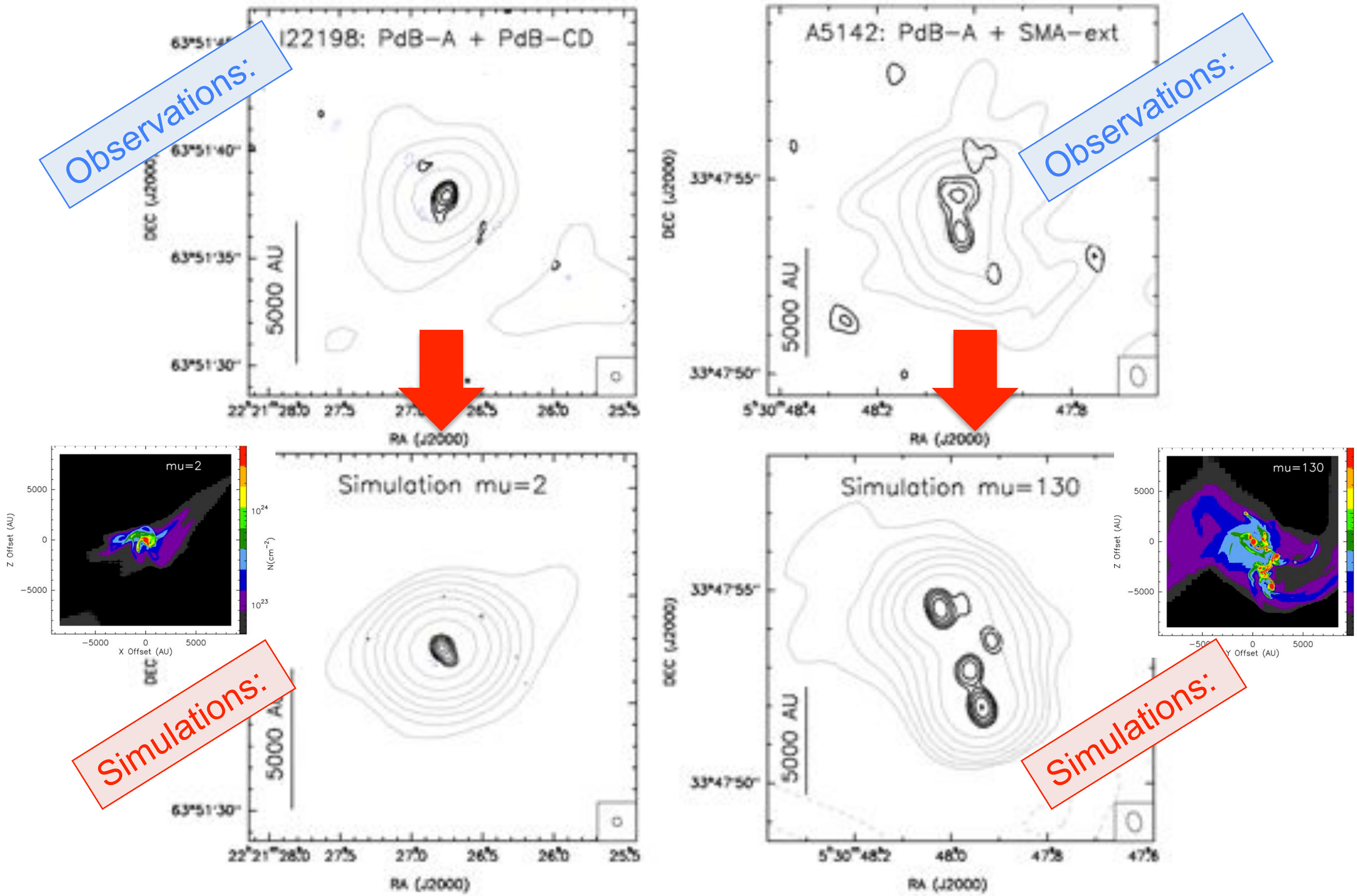

Palau et al. 2013, ApJ, 762, 120

Compare density profiles

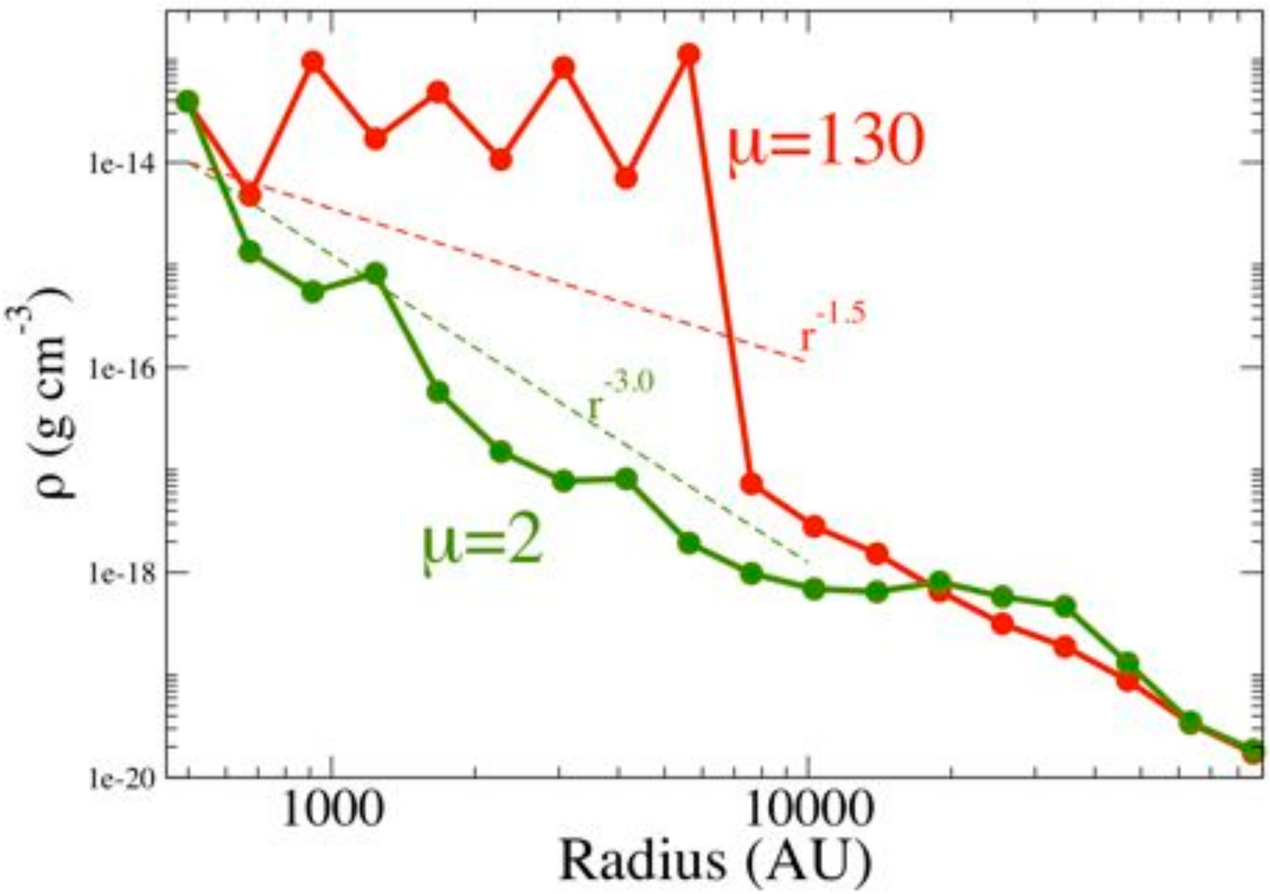

Red line: μ=130

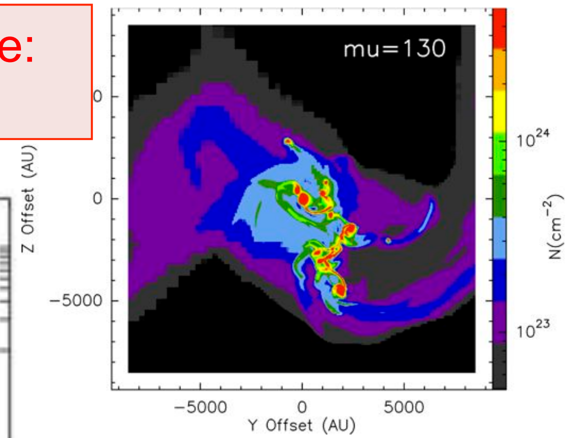

Green line: μ=2

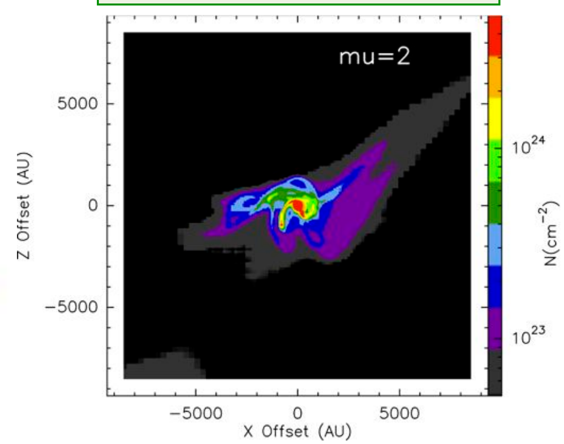

Palau et al. 2014, ApJ, 785, 42

Compare density within 0.1 pc

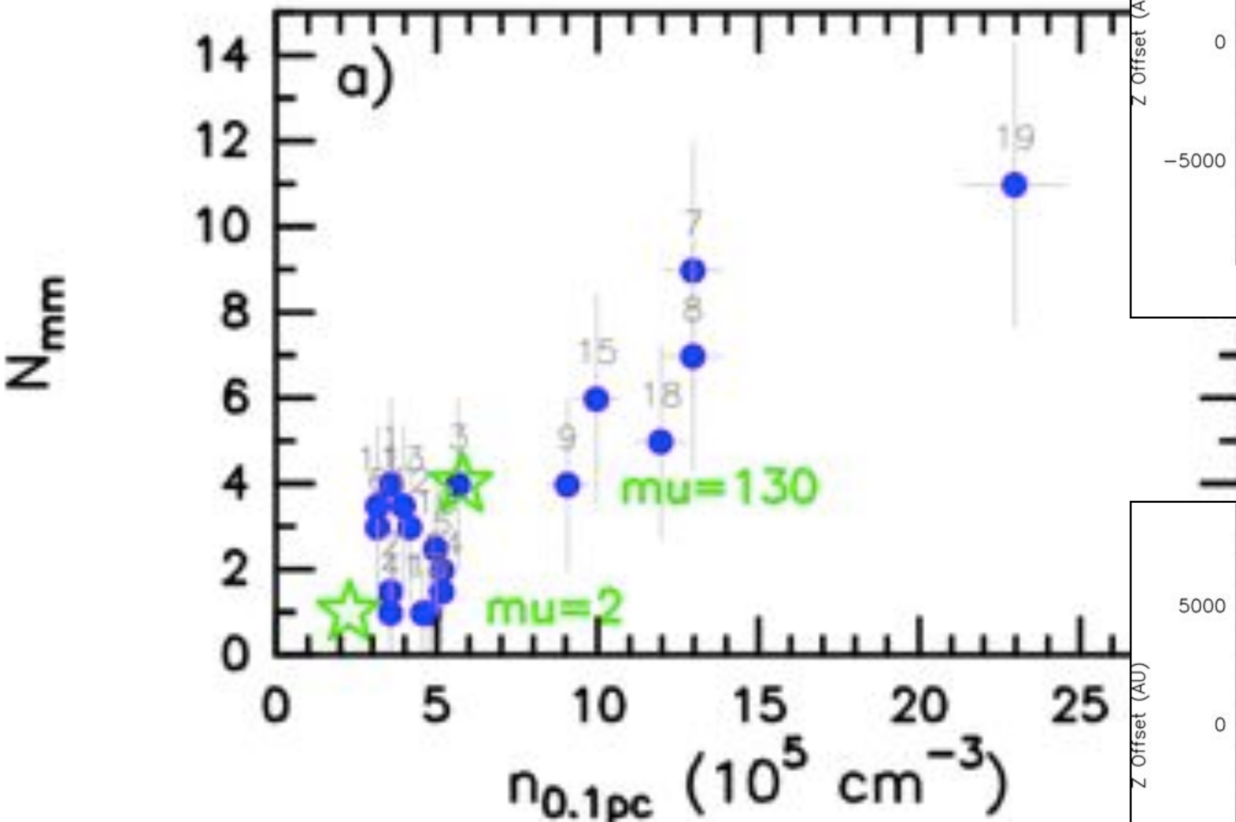

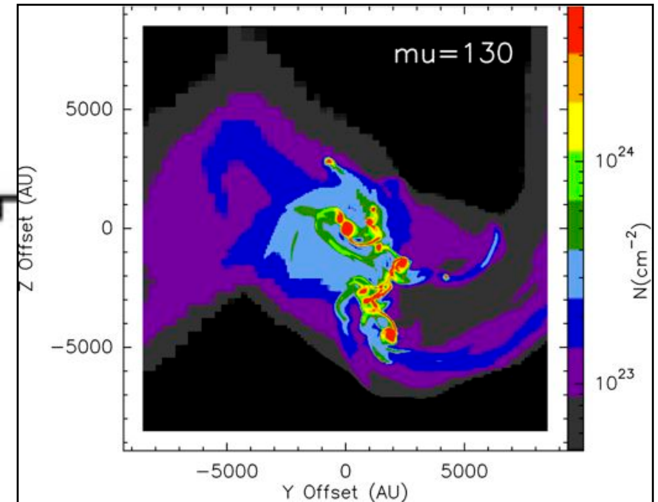

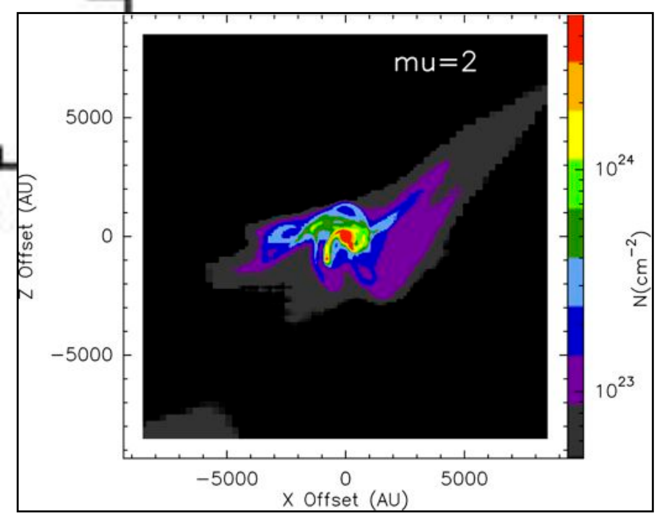

Palau et al. 2014, ApJ, 785, 42

Need to constrain B from observations

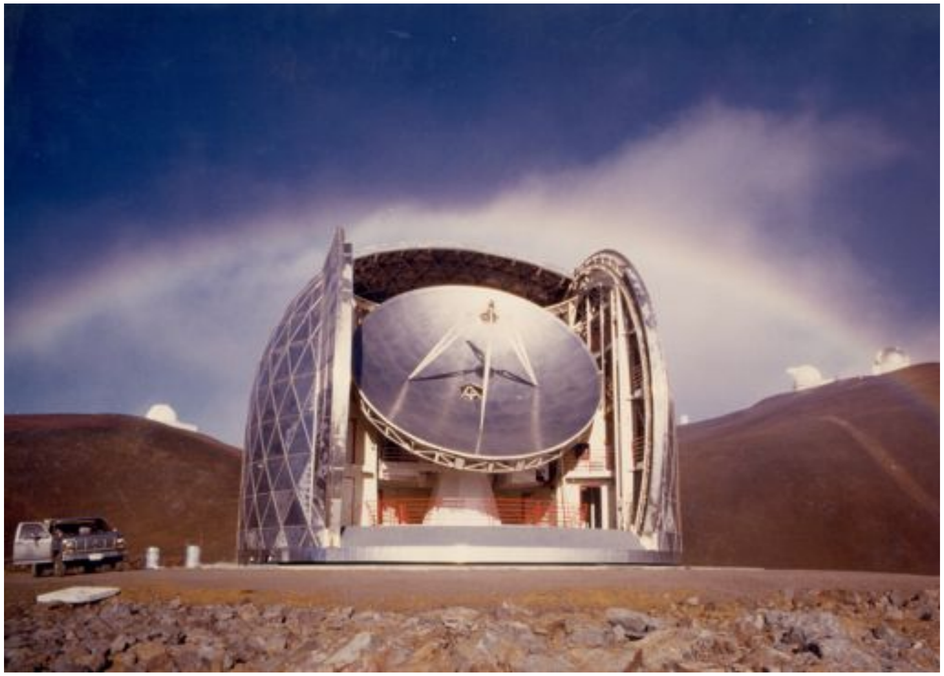

CSO, Hawaii
Palau et al., in prep.

SMA, Hawaii
Palau et al., in prep.

Observations of polarized submm emission: work in progress

Conclusions

- ✓sample of 19 massive dense cores: study fragmentation level vs several properties of the cores

- ✓**data seem to be better described by pure thermal Jeans fragmentation**

- ✓**B potentially helps form concentrated profiles and smaller densities inside a given radius**

Thanks!

$$\left[\frac{M_{\rm Jeans}^{\rm th}}{M_\odot}\right] = 0.6285 \left[\frac{T}{10\,{\rm K}}\right]^{3/2} \left[\frac{n}{10^5\ {\rm cm}^{-3}}\right]^{-1/2}$$

T fixed at 20 K
T calculated from model (avg in 0.1pc)